

THE AGASA AND SUGAR ANISOTROPIES AND TeV GAMMA RAYS FROM THE GALACTIC CENTER: A POSSIBLE SIGNATURE OF EXTREMELY HIGH ENERGY NEUTRONS

ROLAND M. CROCKER,^{1,2} MARCO FATUZZO,³ J. R. JOKIPII,⁴ FULVIO MELIA,⁵ AND RAYMOND R. VOLKAS²

Received 2004 August 6; accepted 2004 December 8

ABSTRACT

Recent analysis of data sets from two extensive air shower cosmic-ray detectors shows tantalizing evidence of an anisotropic overabundance of cosmic rays toward the Galactic center region that “turns on” around 10^{18} eV. We demonstrate that the anisotropy could be due to neutrons created in the Galactic center region through charge exchange in proton-proton collisions, where the incident, high-energy protons obey a $\sim E^{-2}$ power law associated with acceleration at a strong shock. We show that the normalization supplied by the gamma-ray signal from EGRET GC source 3EG J1746–2851 (ascribed to p - p -induced neutral pion decay at GeV energies), together with a very reasonable spectral index of 2.2, predicts a neutron flux at $\sim 10^{18}$ eV fully consistent with the extremely high energy cosmic-ray data. Likewise, the normalization supplied by the very recent GC data from the HESS air Cerenkov telescope at \sim TeV energies is almost equally compatible with the $\sim 10^{18}$ eV cosmic-ray data. Interestingly, however, the EGRET and HESS data appear to be themselves incompatible. We find a plausible resolution of this discrepancy in an *effective* two-source model. Finally, we argue that the shock acceleration is probably occurring in the shell of Sagittarius A East, an unusual supernova remnant located very close to the Galactic center. In support of this contention we note that (1) the extended shell of this object could provide both of the sources suggested by the gamma-ray data and (2) the unusually strong magnetic field at this remnant, together with a perpendicular shock geometry, allow for acceleration of protons up to the extreme energies required to explain the cosmic-ray anisotropy. If the connection between the anisotropy and Sagittarius A East could be firmly established, it would be the first direct evidence for a particular Galactic source of cosmic rays up to energies near 10^{19} eV.

Subject headings: acceleration of particles — cosmic rays — Galaxy: center — radiation mechanisms: nonthermal — supernova remnants

1. INTRODUCTION

The origin of cosmic rays (CRs) is one of the most important unsolved problems in astrophysics. While it has long been speculated that diffusive shock acceleration of protons and ions at shock fronts associated with supernova remnants (SNRs) is the mechanism likely responsible for accelerating the bulk of high-energy CRs, definitive observational proof has been elusive. Further, the conditions at almost all known SNRs seem not to promote the acceleration of CRs beyond the “knee” feature in the spectrum at $\simeq 5 \times 10^{15}$ eV. The acceleration mechanism for CRs between the knee and the “ankle” at a few times 10^{19} eV therefore seems to be an even deeper puzzle.

The purpose of this paper is to argue that the Galactic center (GC) region, given its relatively extreme conditions compared to the rest of the Milky Way, is a likely site for the acceleration of CRs up to the ankle (at $\sim 3 \times 10^{19}$ eV). Our argument is based on the following: (1) The EGRET gamma-ray source 3EG J1746–2851, most likely located in the GC region (although probably not actually *at* the GC), provides good evidence for

pion production from high-energy proton-proton (p - p) collisions. Neutrons will then inevitably also be produced by this source. (2) The TeV gamma rays from the direction of the GC detected by a number of air Cerenkov telescopes (ACTs), in particular, the HESS instrument, also support the notion that high-energy proton acceleration and collision processes (again, leading inevitably to neutron production) are occurring in this region. (3) The AGASA CR anisotropy for the energy range $10^{17.9}$ – $10^{18.5}$ eV, associated with a flux of 2×10^{-17} $\text{cm}^{-2} \text{s}^{-1}$ (Bossa et al. 2003), is consistent with high-energy neutron emission from the GC. (4) The reanalyzed SUGAR data also reveal an anisotropy for this energy regime from a direction close to the GC. Its measurement of the CR flux from a pointlike source, $(9 \pm 3) \times 10^{-18}$ $\text{cm}^{-2} \text{s}^{-1}$, is broadly (see below) consistent with the determination made on the basis of the AGASA anisotropy data.

If the connection between the anisotropies and Sgr A East could be firmly established, it would be the first identification of a specific source producing high-energy, Galactic CRs and, moreover, would be proven to be an important, possibly unique, contributor to CR acceleration up to the ankle. The southern hemisphere AUGER detector, currently under construction, will test our hypothesis in the relatively near future: it should see a significant point source of $\sim 10^{18}$ eV neutrons at the GC (for lower energies, previous work has shown that a GC neutrino signal should also be seen by a northern hemisphere km^3 neutrino telescope; Crocker et al. 2002).

We extend earlier work on GC CR production in three important ways. First, postulating a GC source of high-energy protons obeying a $\sim E^{-2}$ power law at the source, with normalization fixed by the concomitant (GeV) EGRET gamma-ray

¹ Harvard-Smithsonian Center for Astrophysics, 60 Garden Street, Cambridge, MA 02138; rcrocker@cfa.harvard.edu.

² Research Centre for High Energy Physics, School of Physics, University of Melbourne, Parkville 3010, Australia; r.crocker@physics.unimelb.edu.au, r.volkas@physics.unimelb.edu.au.

³ Physics Department, Xavier University, Cincinnati, OH 45207; fatuzzo@cerebro.cs.xu.edu.

⁴ Department of Planetary Sciences, Lunar and Planetary Observatory, University of Arizona, 1629 East University Boulevard, Tucson, AZ 85721; jokipii@lpl.arizona.edu.

⁵ Physics Department and Steward Observatory, University of Arizona, 933 North Cherry Avenue, Tucson, AZ 85721; melia@physics.arizona.edu.

observations of 3EG J1746–2851, we calculate neutron production through charge exchange $pp \rightarrow nX$ reactions. *Quite non-trivially, we find neutron fluxes consistent with the magnitudes of the AGASA and SUGAR anisotropies.* Second, we likewise show that a simultaneous fit to the (TeV) data supplied by the HESS instrument and the CR anisotropy data is also consistent with the existence of a population of shock-accelerated protons governed by a $\sim E^{-2}$ power law up to extremely high energies. Third, we show that diffusive shock acceleration beyond the knee can occur provided that there is a significant magnetic field component *perpendicular* to the SNR shock propagation direction (i.e., parallel to the shock front). We explain why the special conditions at the GC, especially the higher density of the ambient medium and higher magnetic field, can realize this situation. Finally, we argue that the GC SNR Sgr A East is the most likely specific candidate site for CR acceleration up to the ankle. Note, however, that it is not necessary to identify the specific source for the conclusion italicized above to follow.

Note also that we admit from the start that our model is not consistent with all available data. The data, however, are inconsistent among themselves in the two important instances in which there is disagreement with our model (see §§ 3.3 and 4.6). These instances of disagreement (both discussed in further detail below) are (1) that the SUGAR results indicate a point source offset by 7.5° from the GC (whereas we predict, of course, a source at the position of the GC on the sky) and (2) that the \sim TeV measurements of the gamma-ray flux from the GC (by a number of instruments) appear to be deficient compared to what we would expect. We discuss a number of possible resolutions of this discrepancy, finding the most favorable to hinge on there being two effective GC sources of gamma rays, an idea that has some support from current observations.

The plan of this paper is as follows. In § 2 we discuss the historical lack of direct observational evidence linking SNRs to high-energy CRs and a possible role for astrophysical neutrons in providing such evidence. In § 3 we discuss the evidence for an overabundance of CRs coming from the GC direction and how this overabundance may be explained in terms of either high-energy protons or neutrons generated in the GC region. In § 4 we discuss how high-energy astrophysical neutrons can be generated and how, further, the emissivity of astrophysical neutrons in proton-proton interactions can be related to the emissivity of gamma rays in the same process. We also discuss here the gamma-ray data that we have on the GC region. In § 5 we discuss our fits to the totality of high-energy data we have for the GC (i.e., CR anisotropy data and gamma-ray data at various energies). We discuss various possibilities for a consistent interpretation of all the data, in particular the idea that the data may provide evidence for more than one (effective) source operating in the GC region. In § 6 we consider the plausibility of two known GC astrophysical objects as the sources of the various high-energy GC signals. We find that the SNR Sgr A East is a more likely source than the other candidate we consider, Sgr A*, the accretion disk associated with the supermassive black hole at the dynamical center of the Galaxy. In § 7 we present our conclusions. Finally, in the Appendix we briefly discuss astrophysical shock acceleration in the parallel and perpendicular limits.

2. ORIGIN OF COSMIC RAYS: ROLE OF NEUTRONS

The hypothesis that shocks at SNRs are responsible for the acceleration of CRs over the bulk of the observed spectrum is 50 years old (Shklovskii 1953). Indeed, there is strong, albeit circumstantial, evidence that SNRs do accelerate CRs up to

at least the knee in the spectrum at a few PeV (we set $E_{\text{knee}} \equiv 10^{15}$ eV for definiteness). This evidence comes primarily from two arguments:

1. Supernovae seem to be the only class of Galactic object able to inject the power necessary to maintain the observed CR output of about 10^{48} ergs yr $^{-1}$ (e.g., Longair 1994).

2. The CR spectrum is governed by a power law with spectral index around 2.7. This is close to the universal power law of spectral index ~ 2 theoretically expected from diffusive shock acceleration at the sort of strong shock associated with a supernova blast wave. (Note that this theoretical expectation for spectral indices close to 2, at the source, is observationally confirmed by radio and gamma-ray data from various SNRs.) The difference between these two indices, further, can be compellingly explained as arising from energy-dependent propagation/confinement effects.

However, there is yet no *direct* observational evidence for the SNR-CR connection and certainly no particular SNR has been proven to be a CR source. Further, many researchers have found that their models are pushed to accelerate particles up to E_{knee} . This becomes doubly troubling given the fact that, as emphasized by Jokipii & Morfill (1991), matching the spectra at the knee requires, short of a cosmic conspiracy, that the population of CRs above the knee is closely related to that below the knee. In fact, there are good reasons to think that the bulk of the CRs are Galactic in origin up to the ankle in the spectrum at a few times 10 EeV (1 EeV $\equiv 10^{18}$ eV), not the least of which is that a proton of this energy has a gyroradius the size of the radius of the Galactic disk.⁶

We would therefore like to determine whether it is indeed the case that SNRs can accelerate particles up to energies of 10^{18} – 10^{19} eV. Further, it would be helpful to find evidence that some *particular* object is accelerating particles to these extremely high energies (EHEs).

We obviously need to look for a signal in electrically neutral particles, so that the location of the source is not scrambled by deflection due to the Galactic magnetic field.⁷ There are three main candidates: photons, neutrinos, and neutrons.

EHE photons may reach us over Galactic distance scales (photons with energies near 10^{15} eV are severely attenuated for propagation distances of tens of kiloparsecs by pair production interactions with the CMB background, but for still higher energies their mean free path through this background begins to increase again) and would be a signature of very high energy hadronic interactions. However, for, say, hadronic collisions of primaries with energies close to the ankle, the daughter photons from neutral pion decay would be down by more than an order of magnitude on the energies of these primaries. This means that EHE gamma rays are, at best, an indirect signature of the existence of such primaries. Moreover, neutrinos, another concomitant of hadronic collisions, are similarly reduced in energy and, in any case, fluxes at 10^{17} and 10^{18} eV are expected to be orders of magnitude too small to be seen by future km 3 neutrino telescopes. Although three of us have previously shown that the GC should emit neutrinos (Crocker et al. 2000, 2002; see also Alvarez-Muñiz & Halzen 2002), their detection could not settle

⁶ However, higher energy CRs may therefore no longer be confined to our Galaxy and so are almost certainly extragalactic. The upturn in the spectrum at the ankle is nicely consistent with a new population taking over from a diminishing Galactic component.

⁷ Charged particles can still be used for very close sources. See, for example, Chilingarian et al. (2003) for a study of putative CR emission from the 300 pc distant Monogem ring SNR.

the question of where the 10^{18} eV CRs are coming from because the detectable flux of neutrinos lies at considerably lower energies.

This leaves us with neutrons. As for neutrinos and gamma rays, neutrons are an inescapable concomitant of hadronic acceleration of protons and ions: charge exchange occurs in a non-negligible fraction of all interactions between accelerated protons and ambient protons. Neutrons are also produced in p - γ collisions and dissociations of accelerated ions (see below). Furthermore, leading neutrons are produced with a much larger fraction of the incoming proton's energy than either photons or neutrinos and are, therefore, a much more direct signature of the presence of such primaries. The neutron, however, is unstable in free space, a fact we have to take into account when contemplating neutron astronomy.

The neutron is the longest lived unstable “elementary” particle with a decay time at rest, τ_n , of 886 s (Hagiwara et al. 2002). This means that a neutron will travel, on average, a distance of

$$d_n(E_n) = c\gamma_n\tau_n \simeq 9\left(\frac{E_n}{\text{EeV}}\right) \text{ kpc} \quad (1)$$

(where the Lorentz factor is given by $\gamma_n \equiv E_n/m_n$) in free space before decaying. What plausibly neutron-producing regions lie within the ~ 9 kpc distance traveled on average by an EeV neutron? The GC, one of the most energetic regions in the Galaxy, at a distance of around 8.5 kpc is the principal candidate.

What would be a smoking gun signature for EHE CR neutrons? It is in extensive air showers (EASs) apparently initiated by particles coming from the direction of the GC that one would need to look for GC neutrons. The signal might be very difficult to disentangle, essentially because any neutron-initiated EAS at these energies is likely to be indistinguishable from a background, proton-initiated EAS⁸ (which proton, given the presence of the Galactic magnetic field, might originate from a source considerably away from the GC). The best evidence for GC neutrons one might hope for, then, is an *anisotropy* in the EeV CR data in the form of an excess toward the GC. Intriguingly, there is tantalizing evidence, which we now briefly review, from two different data sets that just such an anisotropy exists.

3. THE GALACTIC CENTER ANISOTROPY EXPLAINED BY A GC SOURCE OF PROTONS/NEUTRONS

Recent analysis of data from two different CR detectors has revealed the presence of an anisotropic overabundance of CRs coming from the general direction of the GC. Consistent with these findings, analysis of data from a third array has found a broad anisotropy along the Galactic plane. We now briefly review each of these findings.

Statistically, the most robust determination for an anisotropy has been by the Akeno Giant Shower Array (AGASA) group (Hayashida et al. 1999a), which, in analysis of 114,000 air showers, found a strong (4% amplitude) anisotropy in the energy range $10^{17.9}$ – $10^{18.3}$ eV (we label the $10^{17.9}$ eV energy at which the anisotropy apparently “turns on” E_{onset}). Note that

⁸ Note here, however, that there is a theoretical possibility, at least, that empirical data may one day be able to directly distinguish EHE CR neutrons from protons via characteristic differences between the μ^+ to μ^- ratios seen in the extensive air showers generated by these particles (a proton will produce an excess of π^+ and, therefore, μ^+ in the forward region whereas a neutron will produce an excess of π^- and, therefore, μ^-).

the AGASA Collaboration (Takeda 1999) has estimated that the systematic uncertainty in its instrument's energy calibration is 30%, and so we adopt this figure in our analysis. The group's two-dimensional analysis of the data showed that this anisotropy could be interpreted as an excess of air showers from two regions each of $\sim 20^\circ$ extent, one of 4σ significance near the GC and another of 3σ in Cygnus. Subsequent reanalysis by the AGASA group, incorporating new data, has only served to bolster the claim that the anisotropy is real (Hayashida et al. 1999b) with, this time, a 4.5σ excess seen near the GC over a beam size of 20° between $10^{18.0}$ and $10^{18.4}$ eV.

Prompted by the AGASA result, Bellido et al. (2001) reanalyzed the data collected by the SUGAR CR detector that operated from 1968 to 1979 near Sydney. Setting a priori an energy range similar to that determined for the AGASA anisotropy, these researchers also found an anisotropy, consistent with a point source located at 7.5° from the GC, and 6° from the AGASA maximum over an energy range of $10^{17.9}$ – $10^{18.5}$ eV.

Finally, the HiRes Collaboration has seen a Galactic plane enhancement in CR events in the energy range between $10^{17.3}$ and $10^{18.5}$ eV with 3.2σ confidence (Bird et al. 1999; this is consistent with the AGASA and SUGAR results because the HiRes study was broad scale and did not attempt to pin down whether any particular Galactic longitudes were responsible for the detected excess; Bellido et al. 2001).

As we shortly set out, the anisotropies mentioned above have what we believe is a natural explanation in terms of neutron emission from the GC region (see § 3.2). Before we discuss this idea in detail, however, we also consider the possibility that the observed anisotropies can be explained directly by a diffusive flux of charged particles from the GC. We label such scenarios “GC charged particle models.”

3.1. GC Charged Particle Models

There has been a concerted effort to model the propagation of charged particles from an assumed source in the vicinity of the GC, through various assumed configurations of the Galactic magnetic field, to Earth to see whether these models can reproduce the observed anisotropies (Clay et al. 2000; Bednarek et al. 2002; Candia et al. 2002b). In general, researchers have found that a fair degree of correspondence between models and reality can be achieved, with, in particular, an anisotropy becoming evident for $\mathcal{O}(\text{EeV})$ protons propagating through various field configurations with a magnetic field amplitude of $\mathcal{O}(\mu\text{G})$. Finding an exact correspondence for “turn-on” and “turn-off” energies seems, however, to require quite a bit of fine-tuning of the particulars of \mathbf{B}_{Gal} and is not such a *robust* solution as the neutron idea. Further, for reasonable amplitudes of \mathbf{B}_{Gal} modeling studies show that the actual separation seen between the GC and the observed excess will exceed the $\mathcal{O}(10^\circ)$ observed (Candia et al. 2002a). In fact, Medina-Tanco & Watson (2001) report that the source must be within ~ 2 kpc of Earth to reproduce the observed deflection. This is, of course, a possibility, but then the near alignment with the anisotropies and the GC becomes, essentially, a coincidence. Finally, and perhaps most tellingly, the (consistent with) pointlike anisotropy seen in the SUGAR data is very difficult to reproduce in modeling of charged particle trajectories because the particles tend to smear out until rather higher energies (for reasonable magnetic fields) than E_{onset} .

3.2. GC Neutron Models

The broad idea that neutron emission from the GC may produce an anisotropy was, to our knowledge, first mooted by

Jones (1990). The neutron idea was subsequently revived by the AGASA group in the paper announcing their discovery of the GC anisotropy (Hayashida et al. 1999a). The AGASA paper authors pointed out that the anisotropy turn-on at a definite energy of \sim EeV finds a natural explanation in the fact that, as outlined above, this energy corresponds to a gamma factor for neutrons large enough that they can reach us from the GC. Thus, broadly, neutrons below this energy decay in propagation and are then diverted by Galactic magnetic fields. The cessation of the anisotropy above $\sim 10^{18.4}$ eV can be explained as due to either a very steep GC source spectrum or an actual cutoff in the source so that the background takes over again at this energy.

Most recently, the broad idea above has been considerably refined in the work of Bossa et al. (2003), whose basic scenario we follow and now explain. These authors have made detailed propagation calculations following the trajectories of protons from neutrons that decay in flight from the GC or, to be precise, they follow the trajectories of antiprotons leaving Earth and calculate the probability that a decay should occur over the interval during which the antiproton's path points back to the assumed GC source. Using this procedure, they calculate detailed maps of the arrival direction of the combined neutron and proton signal for various values of an assumed Galactic magnetic field that has both a regular and a turbulent component. The Bossa et al. (2003) scenario extends that presented by Medina-Tanco & Watson (2001) in which, essentially, decay protons produced close to Earth arrive from directions close to the GC, whereas those produced in the inner Galaxy arrive preferentially from the directions of the spiral arms (thus also neatly explaining the Cygnus anisotropy) as their trajectories wind around the regular magnetic field lines.

Crucially, the GC, with declination $\delta = -28^\circ$, is outside the field of view of AGASA (which is limited to $\delta > -24^\circ$; Bossa et al. 2003). This provides a natural explanation for the turn-off of the AGASA anisotropy without the need for a source cutoff: at energies $\gtrsim 10^{18.4}$ eV, neutrons do not (on average) decay in flight from the GC but, instead, travel in a straight line from the GC to Earth to produce a pointlike anisotropy *out* of the field of AGASA. Moreover, Bossa et al. (2003) were also able to reproduce the sharp onset of the ASAGA anisotropy at $10^{17.9}$ eV by positing a Galactic magnetic field random component of fairly large amplitude (3 μ G) and also assuming a GC source governed by a spectral index of 2.2. As mentioned above, these researchers also relate the Cygnus region excess seen by AGASA to the GC source with a Galactic magnetic field whose regular component is along the spiral arms (and not just azimuthal). Finally, in the Bossa et al. (2003) scenario, the *magnitudes and morphologies* of the AGASA and SUGAR results were shown to be compatible (*directional* consistency being problematic; see below). In addition to approximate consistency in magnitude, the fact that the AGASA and SUGAR anisotropies are, respectively, diffuse and (consistent with) pointlike finds a natural explanation. Indeed, from the requirement that the source normalization generate the observed 4% amplitude anisotropy of the right ascension first harmonic (and continuing to assume a power-law source spectrum with index 2.2), Bossa et al. (2003) determine that the total luminosity of the GC source over the specified decade in energy is

$$L_{\text{GC}}(10^{17.5} - 10^{18.5}) \simeq 4 \times 10^{36} \text{ ergs s}^{-1}, \quad (2)$$

which implies a direct neutron flux between $10^{17.9}$ and $10^{18.5}$ eV of $2 \times 10^{-17} \text{ cm}^{-2} \text{ s}^{-1}$ (no error range given), which is not very different from the SUGAR result of $(9 \pm 3) \times 10^{-18} \text{ cm}^{-2} \text{ s}^{-1}$.

Bossa et al. (2003) also point out that these two figures need not be exactly equal: protons will be, in general, delayed by many thousands of years with respect to the neutron arrival times, so the source intensity need not be exactly the same when the neutrons and protons we observe today were separately emitted.

A couple of important points one should note about the Bossa et al. (2003) scenario (as these researchers themselves remark) are that (1) for the magnetic field adopted, the phase ($\sim 330^\circ$) of the first harmonic in right ascension found is somewhat larger than that detected by AGASA; and (2) because Bossa et al. (2003) *do* relate the Cygnus excess to a GC source, this excess should disappear for $E \gtrsim 2$ EeV *independently of the intrinsic source energy cutoff* because any reasonable Galactic magnetic field could not, reasonably, shepherd CRs above this energy along a spiral arm.

3.3. Noncoincidence of the SUGAR Anisotropy with the GC

That the AGASA anisotropy is not exactly coincident with the GC finds a reasonable explanation in the fact already presented that the actual GC is out of the field of view of this instrument. That the SUGAR anisotropy, however, is not coincident with the GC presents a challenge to all scenarios that would posit that the source of the EHE CRs is at the GC. Thus, either all such scenarios are incorrect, or the SUGAR directional determination is somewhat in error. If not the GC, then the SUGAR anisotropy could be due to the SNR W28, which has also been detected by the EGRET instrument in gamma rays. However, W28 (located at $\alpha = 274^\circ$, $\delta = -23^\circ.18$) is itself displaced from the SUGAR position by about 4° , and one would need to again invoke an error in SUGAR's directional determination. For reasons we immediately explain, such an error seems to be a viable possibility. This follows because, if the SUGAR directional determination is correct, then (1) in the case that the anisotropy is due to neutrons, there must be a completely unknown source at the position suggested by the SUGAR data (unobserved, e.g., by the EGRET instrument in gamma rays); or (2) alternatively, in the case that the anisotropy is due to protons directly, either (a) there is a source located very close to us that is constrained to be in close *but completely coincidental* alignment with the direction toward the GC, or (b) there is a source somewhat farther away, the particles produced by which (*also completely coincidentally*) happen to be bent in flight in exactly such a way as to appear to come from close to the direction of the GC (and, further, remain sufficiently bunched that their signal is consistent with pointlike for SUGAR).

We note, furthermore, that whereas, as stressed above, the GC is outside the field of view of AGASA, the position of the SUGAR maximum is *inside* the AGASA field of view so that the putative SUGAR source should be seen by AGASA. That it is not means that *these two instruments are in disagreement*. AGASA, moreover, has the better statistics. Hence we take as a working hypothesis that SUGAR's directional determination is in error. The only other way out of this apparent dilemma is to posit significant variability (between the SUGAR and AGASA observation times) at the source, which, however, would in fact be an argument in favor of a point source, rather than diffuse emission.

4. RELATING GALACTIC CENTER REGION GAMMA-RAY AND NEUTRON SIGNALS

As we explain below, the idea that high-energy hadronic interactions are taking place at the GC is supported by the gamma-ray signals detected from this region. Neutron and gamma-ray

production in proton-proton interactions, moreover, can be related by fairly well understood particle physics. We explain the correlation between the gamma-ray and neutron signals, assuming a common origin in GC proton-proton collisions, in the next section.

4.1. Microphysics of Astrophysical Neutron Production

Being neutral, neutrons may not, of course, be directly accelerated. All high-energy astrophysical neutron production mechanisms, then, require a population of accelerated *charged* particles. Such a charged particle “beam” can, through its impinging on a “target” particle population, produce astrophysical neutrons (with the beam particle indicated first in each pair, the target second) via the following interactions: (1) p - p ; (2) A - p , $A \neq p$; (3) p - γ ; (4) A - γ , $A \neq p$. In more detail, these processes are as follows:

1. Leading neutron production from collisions of accelerated protons with ambient, target protons.
2. Neutron production via dissociation of accelerated ions through collisions with ambient, target protons.
3. Photoproduction of leading neutrons (i.e., charge exchange production of neutrons in collisions of accelerated protons with ambient, target photons).
4. Photodissociation (fragmentation) of accelerated ions.

Of the existing work concerned with the GC anisotropy and its explanation in terms of neutron production at various possible GC sites, the AGASA group’s anisotropy discovery paper (Hayashida et al. 1999a) focused on the idea that the disintegration of accelerated heavy ions by interactions with ambient matter or photons was the ultimate source of the (putative) EHE neutrons. This follows the lines of the broad scenario investigated by Sikora et al. (1989) for active galactic nuclei (AGNs) in which the very same strong magnetic fields that serve to accelerate charged particles to high energies also serve to confine the same to some central accelerating region (whereas neutrons escape). Also of relevance here is the work of Tkaczyk (1994).

Alternatively to the heavy-ion disintegration idea, Medina-Tanco & Watson (2001) have proposed that a more likely method of EHE neutron production is via interactions between accelerated protons and ambient protons or IR photons. They found that the environment of Sgr A*, the supermassive black hole at the GC, is sufficiently dense that the particle interaction rate required to produce the desired neutron flux is achievable. We discuss this scenario further below.

Takahashi & Nagataki (2001) also considered neutron production and determined that it is p - p interactions that most effectively produce the required neutrons. For reasons explained below, we agree with this conclusion (although our calculations differ importantly in specifics). Takahashi & Nagataki (2001) also researched the detectability of neutrinos concomitant with neutron production. More recently, Anchordoqui et al. (2004) have studied the detectability of neutrinos produced in the decay in flight of the (putative) GC neutron beam, and Biermann et al. (2004) have considered a model in which the observed anisotropy is explained as due to the last gamma-ray burst to go off in the Galaxy.

4.2. Galactic Center Region Gamma-Ray Observations: Independent Evidence for Hadronic Acceleration

Independent evidence of hadronic acceleration in the GC region comes from the EGRET detection of a 30 MeV–10 GeV continuum source (3EG J1746–2851 in the third EGRET cat-

alog; Hartman et al. 1999) within 1° of the nucleus (Mayer-Hasselwander et al. 1998).⁹ The EGRET spectrum exhibits a clear break at ~ 1 GeV and therefore cannot be fitted by a single power law. Instead, this break appears to be the signature of a process involving pion decays. Specifically, the decay of neutral pions generated via p - p scatterings between relativistic and ambient protons produces a broad gamma-ray feature that mirrors all but the lowest energy EGRET data. Of course, p - p scatterings also produce charged pions that, in turn, decay into “secondary” electrons and positrons. These leptons are capable of producing their own gamma-ray emission via bremsstrahlung and Compton scattering. Interestingly, if the secondary leptons build up to a steady state distribution balanced by bremsstrahlung and Coulomb losses, the former accounts naturally for the lowest energy EGRET datum, *independent of the ambient proton number density*. This crucial feature results from the fact that the secondary leptons produce a steady state distribution whose normalization scales as the inverse of the ambient proton number density, whereas the bremsstrahlung emissivity per lepton scales directly with this density. The pion decays link the lepton and photon generation rates, so the bremsstrahlung and pion-decay photon emissivities are tightly correlated.

While this discussion is quite general in nature, it is important to note that Sgr A East, a mixed-morphology SNR located within several parsecs of the Galactic center, is a viable candidate for the site of hadronic acceleration (see § 6.2 for a more complete discussion). Specifically, the observation of OH maser emission at the boundary of this structure provides strong evidence for the presence of shocks (Yusef-Zadeh et al. 1996, 1999). In addition, Fatuzzo & Melia (2003) have found that a power-law distribution of shock-accelerated relativistic protons injected into the high-density, strongly magnetized Sgr A East environment leads to a pion-decay process (described above) that can account for both the EGRET source 3EG J1746–2851 and the unique radio characteristics of Sgr A East. This scenario may also account for the e^+e^- annihilation radiation observed from the Galactic bulge by the Oriented Scintillation Spectrometer Experiment (OSSE) aboard the *Compton Gamma Ray Observatory* (Fatuzzo et al. 2001).

Finally, further evidence for the occurrence of hadronic acceleration at the Galactic center is presented by the detection of this region at \sim TeV energies by a number of ACTs (see § 4.6 for more on this point).

4.3. Detailed Calculation of Neutron Flux from p - p Collisions

Given, now, a population of protons accelerated to relativistic energies at the GC source, these can undergo a series of interactions including $pN \rightarrow pNm_{\text{meson}}m_{N\bar{N}}$, where N is either a p or a neutron n , m_{meson} denotes the energy-dependent multiplicity of mesons (mostly pions), and $m_{N\bar{N}}$ is the multiplicity of nucleon/antinucleon pairs (both increasing functions of energy). Since $m_{N\bar{N}}/m_{\text{meson}} < 10^{-3}$ at low energy and even smaller at higher energies (Cline 1988), following Markoff et al. (1997), we here ignore the antinucleon production events.

Note that the charge exchange interaction ($p \rightarrow n$) occurs around 40% of the time at accelerator energies (Dao et al. 1974; Engler et al. 1975; Flauger & Mönning 1976; Blobel et al. 1978; Forti et al. 1990; Frichter et al. 1997) and this fraction is predicted by Gribov-Regge theory and Monte Carlo modeling to be only very weakly energy dependent (Capdevielle et al. 1992;

⁹ The IBIS telescope on board *INTEGRAL* has also recently released a preliminary result for the detection of a GC source in the EGRET energy range (Di Cocco et al. 2004).

Capdevielle & Attallah 1992; Werner 1993; Engel 2001; Huang et al. 2002; Ostapchenko 2003). Hence, we take the *leading* neutron multiplicity, m_n , to be given by a fixed proportion of 0.4 (i.e., 40% of all p - p interactions involve charge exchange, independent of incoming proton energy). Further, the highest energy experimental data available indicate, for p - p interactions, an averaged leading neutron elasticity of $\langle x_n \rangle = 0.25$ (Frichter et al. 1997).

Other possible interactions of accelerated protons, all potentially important for cooling, are $p\gamma \rightarrow p\pi^0\gamma$, $p\gamma \rightarrow n\pi^+\gamma$, $p\gamma \rightarrow e^+e^-p$, and $pe \rightarrow eNm_{\text{meson}}$ (Markoff et al. 1997).

4.3.1. The Production of π^0 -Decay Photons

The (differential) π^0 emissivity resulting from an isotropic distribution of shock-accelerated protons $dn_p(E_p)/dE_p$ (where $[dn_p(E_p)/dE_p]$ is in units of $\text{cm}^{-3} \text{eV}^{-1}$) interacting with cold (fixed target) ambient hydrogen of density n_H is given by the expression

$$Q_{\pi^0}^{pp}(E_{\pi^0}) = cn_H \int_{E_p^{\text{th}}(E_{\pi^0})} dE_p \frac{dn_p(E_p)}{dE_p} \frac{d\sigma(E_{\pi^0}, E_p)}{dE_{\pi^0}}, \quad (3)$$

where $E_p^{\text{th}}(E_{\pi^0})$ is the minimum proton energy required to produce a pion with total energy E_{π^0} (determined through kinematical considerations) and $[Q_{\pi^0}^{pp}] = \text{pions s}^{-1} \text{cm}^{-3} \text{eV}^{-1}$. The resulting gamma-ray emissivity is then given by the expression

$$Q_\gamma(E_\gamma) = 2 \int_{E_{\pi^0}^{\text{min}}(E_\gamma)} dE_{\pi^0} \frac{Q_{\pi^0}^{pp}(E_{\pi^0})}{(E_{\pi^0}^2 - m_{\pi^0}^2)^{1/2}}, \quad (4)$$

where $E_{\pi^0}^{\text{min}}(E_\gamma) = E_\gamma + m_{\pi^0}^2/(4E_\gamma)$.

At proton energies, E_p , greater than ~ 5 GeV, above the Δ resonance-affected region, the differential cross section is approximated by the scaling form of Blasi & Melia (2003; see also Blasi & Colafrancesco 1999):

$$\frac{d\sigma(E_p, E_{\pi^0})}{dE_{\pi^0}} = \frac{\sigma_0}{E_{\pi^0}} f_{\pi^0}(x_0), \quad (5)$$

where $x_0 \equiv E_{\pi^0}/E_p$, $\sigma_0 = 32$ mbarn, and (Hillas 1980)

$$f_{\pi^0}(x_0) = 0.67(1 - x_0)^{3.5} + 0.5e^{-18x_0}. \quad (6)$$

This scaling form properly takes into account the high pion multiplicities that occur at high energies.

Given the above and a parent proton distribution governed by a power law $dn_p(E_p)/dE_p$ with spectral index γ ,

$$\frac{dn_p(E_p)}{dE_p} \propto E_p^{-\gamma}, \quad (7)$$

we can write the neutral pion emissivity due to p - p as

$$Q_{\pi^0}^{pp}(E_{\pi^0}) = \frac{dn_p(E_{\pi^0})}{dE_p} \sigma_0 n_H c \Lambda^0(\gamma) \quad (8)$$

and, consequently, the photon emissivity due to the decay of these π^0 as

$$\begin{aligned} Q_\gamma(E_\gamma) &\simeq cn_H \int_{E_\gamma}^\infty dE_{\pi^0} \int_{E_{\pi^0}}^\infty dE_p \frac{dn_p(E_p)}{dE_p} \frac{d\sigma(E_p, E_{\pi^0})}{dE_{\pi^0}} \frac{2}{E_{\pi^0}} \\ &\simeq \frac{2}{\gamma} \frac{dn_p(E_\gamma)}{dE_p} \sigma_0 n_H c \Lambda^0(\gamma), \end{aligned} \quad (9)$$

where in both equations immediately above we employ

$$\begin{aligned} \Lambda^0(\gamma) &\equiv \int_0^1 dx_0 x_0^{\gamma-2} f_{\pi^0} \\ &= 2 \left\{ \Gamma(\gamma - 1) \left[18^{1-\gamma} + \frac{15.5865}{\Gamma(3.5 + \gamma)} \right] - E(2 - \gamma; 18) \right\}, \end{aligned} \quad (10)$$

in which $\Gamma(x)$ is the Euler gamma function and $E(n; z)$ is the exponential integral function that satisfies $E(n; z) \equiv \int_1^\infty \exp(-zt)/t^n dt$.

4.3.2. The Production of Neutrons in the Scaling Regime

As above, the emissivity of neutrons from an isotropic distribution of shock-accelerated protons $dn_p(E_p)/dE_p$ interacting with cold (fixed target) ambient hydrogen of density n_H is given by the expression

$$Q_n^{pp}(E_n) = cn_H \int_{E_p^{\text{th}}(E_n)} dE_p \frac{dn_p(E_p)}{dE_p} \frac{d\sigma(E_n, E_p)}{dE_n}. \quad (11)$$

To proceed further, we would like to take, in analogy to the above,

$$\frac{d\sigma(E_p, E_n)}{dE_n} = \frac{\sigma_0}{E_n} f_n(x_n), \quad (12)$$

where $x_n \equiv E_n/E_p$. We must now determine an expression for $f_n(x_n)$. In this regard, we employ the formalism set out in Appendix A of Drury et al. (1994). Following Gaisser (1990), this reference sets out the calculation of the ‘‘spectrum-weighted moment’’ (SWM), denoted by $\langle mx_S \rangle_S^\gamma$, for the emission spectrum of various particle species (labeled by S) from collisions of protons from a power-law distribution equation (7) and where $x_S \equiv E_S/E_p$. In this formalism, the emissivity of species S can be written

$$Q_S(E_S) = \frac{dn_p(E_S)}{dE_p} \sigma_{pp} n_H c \langle mx_S \rangle_S^\gamma, \quad (13)$$

so that we see that $\Lambda^0(\gamma)$ defined in equation (10) above is nothing but the SWM for neutral pions produced in p - p collisions.

Drury et al. (1994) provide their own calculation of the SWM for neutral pions, decay gammas, and neutrons ($\langle mx_{\pi^0} \rangle_{\pi^0}^\gamma$, $\langle mx_\gamma \rangle_\gamma^\gamma$, and $\langle mx_n \rangle_n^\gamma$). We set out their results and ours (calculated with the f_{π^0} given above) for comparison for pions and pion-decay gammas in Table 1.

To arrive at an SWM for neutron production calculations, Drury et al. (1994) employ the dimensionless, inclusive cross section for neutron production given by Jones (1990), viz.,

$$g_n(x_n) = n_n(\alpha_n + 1)(1 - x_n)^{\alpha_n}. \quad (14)$$

TABLE 1
VALUES OF $\Lambda(\gamma)$ FOR BOTH NEUTRAL PIONS AND NEUTRONS FROM p - p COLLISIONS
COMPARED TO THE SPECTRUM-WEIGHTED DISTRIBUTIONS FOR THE SAME
CALCULATED IN DRURY ET AL. (1994)

γ	$\Lambda^0(\gamma)$	$\langle mx_{\pi^0} \rangle_{\pi^0}^\gamma$	$\Lambda^n(\gamma)$	$\langle mx_n \rangle_n^\gamma$
2.0.....	0.177	0.17	0.177	0.19
2.2.....	0.113	0.092	0.103	0.094
2.4.....	0.076	0.066	0.063	0.051
2.6.....	0.053	0.048	0.041	0.030

Jones (1990) gives, on the basis of his analysis of 300 GeV proton collider data, $\alpha_n = 2$ and an average neutron multiplicity, n_n , of 0.25. We adopt his results excepting the neutron multiplicity, which we revise to be 0.4 as set out above. We find, then, that

$$g_n(x_n) \rightarrow 1.2(1 - x_n)^2. \tag{15}$$

The translation of this distribution into our formalism is simply

$$f_n(x_n) \equiv x_n g_n(x_n) = 1.2x_n(1 - x_n)^2. \tag{16}$$

We find, then,

$$Q_n^{pp}(E_n) \simeq cn_H\sigma_0 \frac{dn_p(E_n)}{dE_p} \Lambda^n(\gamma), \tag{17}$$

where we have defined

$$\Lambda^n(\gamma) \equiv \int_0^1 dx_n x_n^{\gamma-2} f_n(x_n) = 2.4 \frac{1}{\gamma(\gamma+1)(\gamma+2)}. \tag{18}$$

4.3.3. Relating Photon and Neutron Emissivity and Fluxes in the Scaling Regime

Now, from equations (9) and (17) we have that

$$Q_n^{pp}(E_n) = \frac{\gamma}{2} \frac{\Lambda^n(\gamma)}{\Lambda^0(\gamma)} Q_\gamma(E_\gamma^0) \left(\frac{E_n}{E_\gamma^0}\right)^{-\gamma}, \tag{19}$$

where we have also used the fact that both daughter γ and neutron spectra will be governed by the same power law as the parent protons. We have, then, related the neutron emissivity at some energy E_n to the photon emissivity at a normalization energy E_γ^0 (assuming that scaling holds). We present $(0.8\gamma\Lambda^n[\gamma])/\Lambda^0[\gamma]$ for various values of the spectral index γ in Table 2. The growth of this ratio with energy can be related to the fact that, because the average energy of a neutron produced in a p - p interaction (at lab energy E_p) will be higher than the energy of a pion-decay gamma produced (indirectly) by a p - p interaction at the same energy (E_p), the neutron flux at E_n is “directly” tied to the photon flux at a somewhat lower energy. This means that as one steepens a spectrum, thereby increasing the number of photons in the population below some fixed pivot point (at which the normalization is affected), one also tends to increase the population of neutrons at E_n .

Note that in employing the relation set out in equation (19), careful attention should be paid to the following points:

1. The neutron emissivity is related not to the *total* photon emissivity, but rather to that part of the photon signal due to

pion decay. Determining an expectation, then, for a neutron emissivity or flux requires that one be able to confidently pin down what proportion of the gamma-ray signal at some normalization energy is due to pion decay.

2. In our derivation it was assumed that $f_n(x)$ is given by its scaling form. This means that photon emissivity (or flux) data must be taken from observations made at sufficiently high energy that we are guaranteed to be in the scaling regime, viz., above ~ 5 GeV.

3. Likewise, it is assumed that the neutrons scale as indicated by equation (16). This relation can be expected to go wrong at sufficiently high energies (see below for more on this point). Note that we are concerned with p - p interactions at a lab energy of $\sim 5 \times 10^{18}$ eV, entailing a center-of-mass system energy range of $s^{1/2} \sim 70$ TeV.

4. The parent proton power law will cut off at sufficiently high energy. In making predictions for neutron flux, one must check that one is not above this cutoff energy.

4.4. The Production of Neutrons at EHE: Accounting for Cross Section Scaling Violation

The above technology allows us to relate the neutron emissivity to the photon emissivity of the same astrophysical object *provided that scaling holds*. That this caveat obtains can be seen directly from the fact that the integral of equation (12) over E_n , which should define the inclusive cross section for neutron production, is, in fact, independent of center-of-mass energy. This approximation holds good, by definition, over the scaling regime from, say, 10 to 1000 GeV for the incident proton energy in the lab frame, but at the lab energies of over 10^9 GeV that we are concerned with for EHE neutron production, it is no longer accurate (see Hagiwara et al. 2002, Fig. 39.12). To the level of accuracy required for the current application, however, it is not too difficult to account for the cross section growth. To render the logic here most perspicuous, the process can be described as a two-step one: (1) relate, via equation (19), the photon and neutron emissivities at an energy scale small enough that scaling holds and the cross section can be taken to be constant with respect to center-of-mass energy, and (2) relate the high-energy neutron emissivity to the low-energy neutron emissivity (inside the scaling regime) via the assumed power-law distribution and the ratios of the total p - p cross sections at these two energy regimes, $\sigma_{pp}(E_n)/\sigma_{pp}(E_\gamma)$.

4.5. Neutron and Gamma-Ray Fluxes Related Given Neutron Decay

Of course, we can equally well relate the observed pion-decay gamma-ray flux at Earth to the expected neutron flux (neglecting neutron decay, as well as other effects that might treat photons and neutrons differently in propagation, for the moment). Indeed, one may quickly determine that, given a power-law parent proton distribution and also accounting for the growth in the total cross section discussed above,

$$F_n^{\text{nd}}(E_n) \simeq \frac{\gamma}{2} \frac{\Lambda^n(\gamma)}{\Lambda^0(\gamma)} F_\gamma(E_\gamma^0) \left(\frac{E_n}{E_\gamma^0}\right)^{1-\gamma} \frac{\sigma_{pp}(\sim 10^{18} \text{ eV})}{\sigma_{pp}(\sim 10^{12} \text{ eV})}, \tag{20}$$

where $F_n^{\text{nd}}(E_n)$ denotes the total flux of neutrons *above* E_n that would be detected at Earth if the neutrons did not decay (super-script nd denotes “no decay”) and $F_\gamma(E_\gamma^0)$ denotes the total flux of π -decay photons detected above the normalization energy

TABLE 2
THE RATIO BETWEEN PHOTON AND NEUTRON EMISSIVITIES
(AT THE SAME ENERGY) FROM p - p COLLISIONS
IN THE SCALING REGIME

γ	$(\gamma\Lambda^n[\gamma])/(2\Lambda^0[\gamma])$
2.0.....	0.566
2.1.....	0.674
2.2.....	0.790
2.4.....	1.072
2.6.....	1.360

TABLE 3
VALUES FOR THE FLUX OF NEUTRONS ABOVE $10^{17.9}$ eV
DUE TO THE EGRET GC SOURCE

γ	Case 1 (neutrons $\text{cm}^{-2} \text{s}^{-1}$)	Case 2 (neutrons $\text{cm}^{-2} \text{s}^{-1}$)
2.1.....	$(1.1^{+1.7}_{-0.7}) \times 10^{-16}$	$(6.1^{+9.9}_{-3.7}) \times 10^{-17}$
2.2.....	$(1.7^{+3.1}_{-1.1}) \times 10^{-17}$	$(9.8^{+17.3}_{-6.1}) \times 10^{-18}$
2.3.....	$(3.0^{+5.6}_{-1.9}) \times 10^{-18}$	$(1.6^{+3.0}_{-1.0}) \times 10^{-18}$
2.4.....	$(4.9^{+9.9}_{-3.2}) \times 10^{-19}$	$(2.6^{+5.2}_{-1.7}) \times 10^{-19}$

NOTES.—For cases in which neutron decay in flight (1) is *not* and (2) is accounted for. These numbers should be compared to the flux calculated “indirectly” from the AGASA data by Bossa et al. (2003), viz., $2 \times 10^{-17} \text{ cm}^{-2} \text{ s}^{-1}$ between $10^{17.9}$ and $10^{18.5}$ eV, and “directly” from the SUGAR data for the observed pointlike excess, viz., $(9 \pm 3) \times 10^{-18} \text{ cm}^{-2} \text{ s}^{-1}$ for the same energy range (Bellido et al. 2001).

E_γ^0 . Note that the above relation, directly relating a neutron flux at Earth to a photon flux at Earth, obviates the need for an accurate estimate of the distance to the source. Also note from Figure 39.12 of Hagiwara et al. (2002) that the ratio of the p - p total cross sections pertinent to the gamma-ray and neutron production regimes is

$$\frac{\sigma_{pp}(\sim 10^{18} \text{ eV})}{\sigma_{pp}(\sim 10^{12} \text{ eV})} \simeq \frac{150 \text{ mbarn}}{40 \text{ mbarn}} = 3.75. \quad (21)$$

We are now in a position to provide a preliminary estimate of the neutron flux above, say, $10^{17.9}$ eV based on the EGRET data on the GC source. From the data provided in Mayer-Hasselwander et al. (1998), the differential flux of photons at $\sim (6.3^{+3.7}_{-2.3}) \times 10^9$ eV is $6 \times 10^{-18} \text{ cm}^{-2} \text{ s}^{-1} \text{ eV}^{-1}$. With a power-law spectrum of spectral index γ this translates to a gamma-ray flux

$$F_\gamma(6.3 \times 10^9 \text{ eV}) = \frac{(3.8^{+3.2}_{-1.8})}{\gamma - 1} \times 10^{-8} \text{ cm}^{-2} \text{ s}^{-1}. \quad (22)$$

Substituting this photon flux into equation (20), we find the values for neutron flux tabulated against γ in the second column of Table 3.

As stressed, however, these preliminary flux estimates do not take into account propagation effects. In this regard, we can quickly dismiss any potential effect from attenuation of the neutrons due to collisions with ambient particles in propagation: here the greatest *potential* effect would be due to collisions of the neutrons with ambient protons (see § 4.7.1). Now, based on extinction at IR and optical wavelengths, the column density to the GC is at most around $5 \times 10^{22} \text{ cm}^{-2}$, implying a “grammage” of matter that must be traversed by the GC neutrons in reaching Earth of around 0.1 g cm^{-2} or less. Neutron energy losses due to interaction with ambient matter in propagation only become significant for grammages in excess of 80 g cm^{-2} (Tkaczyk 1994), however, and are, therefore, entirely negligible in this instance (one can also establish that TeV photons from the GC are not significantly attenuated by pair production in propagation; see § 5.1).

In contrast, neutron decay must certainly be accounted for. We can incorporate this effect by writing the flux as

$$F_n(E_n) \simeq \int_{E_n}^{\infty} \frac{dF_n^{\text{nd}}(E_n)}{dE_n} \exp\left[-\frac{d_{\text{GC}}}{d_n(E_n)}\right] dE_n, \quad (23)$$

where d_{GC} is the distance to the GC, $d_n(E)$ is the neutron mean free path defined in equation (1), and the neutron differential flux without decay is given by (cf. eq. [19])

$$\frac{dF_n^{\text{nd}}(E_n)}{dE_n} \simeq 1.9\gamma \frac{\Lambda^n(\gamma)}{\Lambda^0(\gamma)} \frac{dF_\gamma(E_\gamma^0)}{dE_\gamma^0} \left(\frac{E_n}{E_\gamma^0}\right)^{-\gamma}, \quad (24)$$

in which, as above, E_γ^0 is some normalizing energy at which the π^0 -decay photons are observed and the numerical factors from equations (20) and (21) combine to give $3.75 \times 0.8 = 3.0$. Note that now the distance to the source enters into the calculation. We present the result of calculating the neutron flux with decay in the third column of Table 3.

As one can see from Table 3, the putative neutron source seen (indirectly) by AGASA and (directly) by SUGAR is easily accounted for by the GC EGRET source with a spectral index of $\gamma = 2.2 \rightarrow 2.3$ (the best fit is at 2.23; see § 5.1). Not only is this range fully compatible with the expectation from theoretical calculations of shock acceleration spectra, but it is also completely consistent with the value of 2.2 recently determined by Fatuzzo & Melia (2003) as their best fit for pion-decay gammas to the EGRET source 3EG J1746–2851 (see more on this point below) and, further, is also consistent with the spectral index of 2.2 determined by Bossa et al. (2003) in their fit to the EHE AGASA data.

Note that other possible neutron production channels (besides p - p collisions) are discussed in § 4.7.

4.6. Detection of the Galactic Center Region at TeV Energies

A Galactic center source has been detected by three ACTs at $\mathcal{O}(\text{TeV})$ energies: Whipple (Kosack et al. 2004), CANGAROO (Tsuchiya et al. 2004), and, most recently and significantly, HESS (Aharonian et al. 2004). In addition, the Hegra ACT instrument has put a (weak) upper limit on GC emission at 4.5 TeV (Aharonian et al. 2002) and the Milagro water Cerenkov extensive air shower array has released a preliminary finding of a detection at similar energies from the “inner Galaxy” (defined as $l \in \{20^\circ, 100^\circ\}$ and $|b| < 5^\circ$; Fleysler et al. 2002). Here we address only the Whipple, CANGAROO, and HESS results in any detail, although note that all the observations mentioned above lend crucial support to the notion that acceleration of particles to very high energies is taking place at the GC.

Even restricting ourselves to consideration of results from these three instruments, we find the situation somewhat confused regarding the GC. In fact, it was clear, even before the arrival of the recent, remarkable data from the HESS instrument, that the Whipple and CANGAROO GC observations were in conflict: Whipple has detected (in data collected over a total of 26 hr from 1995 to 2003), at (conservatively) the 3.7σ level, a flux of photons from the GC direction of $(1.6 \pm 0.5 [\text{stat}] \pm 0.3 [\text{sys}]) \times 10^{-12} \text{ cm}^{-2} \text{ s}^{-1}$ above 2.8 TeV (Kosack et al. 2004), which is 40% of the Crab flux above this same energy. (In regards to the errors on the measurement, note that there is a 20% uncertainty, too, in the calibration of the 2.8 TeV energy threshold.) This is to be contrasted with GC data that were collected in 2001 and 2002 by the CANGAROO-II ACT. From these data the CANGAROO collaboration has been able to generate a spectrum for the GC source in six energy bins. From this spectrum can be extracted (Hooper et al. 2004) a flux of around $2 \times 10^{-10} \text{ cm}^{-2} \text{ s}^{-1}$ above 250 GeV. The CANGAROO Collaboration also determined an extremely steep spectrum for their GC source with a fitted photon index of 4.6 ± 0.5 . Given

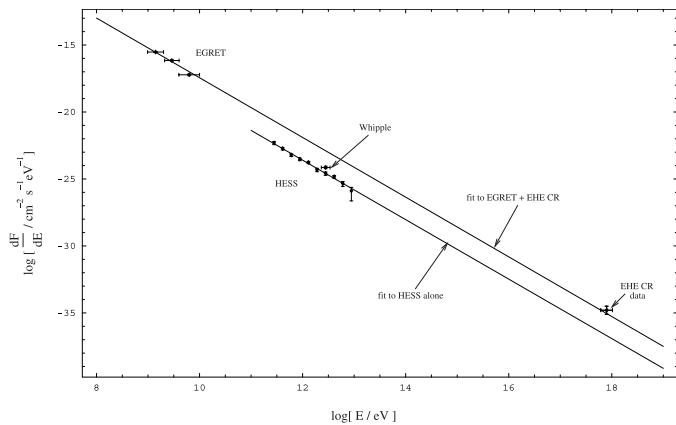


FIG. 1.—Gamma-ray and neutron differential fluxes together with fitted curves. The three points on the left of the figure are from EGRET (Mayer-Hasselwander et al. 1998). The 11 data points in the middle of the figure are GC, gamma-ray differential fluxes measured by atmospheric Cerenkov telescopes. Among these, the single point with marked error bars sitting above the fitted line is due to Whipple (Kosack et al. 2004), while the other 10 points are from the recent HESS 2003 July–August data set (Aharonian et al. 2004). The right data point gives the neutron flux, which, on the basis of the EHE CR data, we have taken to be $(1.0^{+1.0}_{-0.5}) \times 10^{-17} \text{ cm}^{-2} \text{ s}^{-1}$ above $10^{17.9} \text{ eV}$. The upper line gives the best-fit (as described in the text) photon differential flux obtained from a simultaneous fit to the EGRET and EHE CR data. This is given by a power law with a spectral index of 2.23 (the curve would be inaccurate at EHE because it does not take into account the growth of the total $p-p$ cross section). Obscured by (i.e., in excellent agreement with) the right data point is a triangle indicating the position of the neutron differential flux at $10^{17.9} \text{ eV}$ as determined by the best-fit power law (that this point is apparently on top of the gamma-ray flux curve is coincidental). The lower curve, with a spectral index of 2.22, has been found by fitting a power law to the HESS data alone. Note how extremely closely the spectral indices match.

the integral flux and photon index above, the CANGAROO GC source is at the level of 0.1 crab units at 1 TeV or around 15 crab units at 250 GeV (Tsuchiya et al. 2004; a “crab unit” is the integral flux of the Crab Nebula above 1 TeV).

The fluxes of the Whipple and CANGAROO sources (relative to the Crab) are, then, quite different, and a natural reading of the situation is that the instruments are in conflict (for further discussion on this point see Hooper et al. 2004). Note that any variability of the GC source at these energies is now constrained to be small (Kosack et al. 2004) so that, although the two instruments in question collected their GC data over periods largely noncoincident with each other, there is little leeway for explaining the difference between the two instruments by positing that they happened to observe the source at different activity levels. Also note that the fields of view of the two instruments are similar and that their respective GC sources are at similar positions and of similar extent (S. Fegan 2004, private communication).

Adding very significantly to our knowledge of the GC at $\sim \text{TeV}$ energies, the High Energy Stereoscopic System (HESS) Collaboration (Hinton 2004), which employs four imaging atmospheric Cerenkov telescopes, has recently released TeV-range, GC data unprecedented in their detail. This group has detected a signal in observations conducted over two epochs (2003 June–July and 2003 July–August) with a 6.1σ excess evident in the former and a 9.2σ excess in the latter (Aharonian et al. 2004). The data from the larger, 2003 July–August data set (which we use in our analysis) can be fitted by a power law with, from the collaboration’s own determination (Aharonian et al. 2004), a spectral index 2.21 ± 0.09 and normalization $(2.50 \pm 0.21) \times 10^{-8} \text{ m}^{-2} \text{ s}^{-1} \text{ TeV}^{-1}$ with a total flux above the instrument’s 165 GeV threshold of $(1.82 \pm 0.22) \times 10^{-7} \text{ m}^{-2} \text{ s}^{-1}$ (there is also a 15%–20% error from energy resolution un-

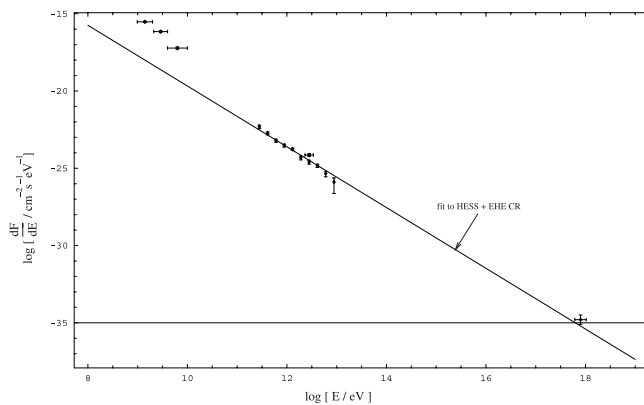


FIG. 2.—Gamma-ray and neutron differential fluxes together with another fitted curve. The data are as given in Fig. 1. The curve is obtained from a power-law fit (simultaneously) to the HESS $\sim \text{TeV}$ gamma-ray data (but not the Whipple data point) and the EHE CR data (again, note that the curve would be inaccurate at EHE because it does not take into account the growth of the total $p-p$ cross section). The best-fit spectral index is 1.97. The EGRET data points have *not* been used in this fit. On the right is illustrated both the EHE CR data point and (again obscured by the former) a triangle indicating the position of the neutron differential flux at $10^{17.9} \text{ eV}$ as determined by the best-fit power law.

certainty). Data from the 2003 June–July run are consistent within errors with the 2003 July–August data.

The HESS flux determination is equivalent to 5% of that from the Crab above the 165 GeV threshold. It is in conflict with the results from Whipple (see Figs. 1 and 2), the latter’s flux determination being a factor of 3 above that implied by the HESS spectrum (Aharonian et al. 2004). It is also in striking conflict with the CANGAROO data: the HESS spectral index determination is clearly at variance with the very steep spectrum found by CANGAROO (for a clear illustration of this fact see Fig. 4 of Aharonian et al. 2004). Again, one might interpret these discrepancies as evidence for significant source variation between the instruments’ different observing periods (i.e., over timescales of $\sim 1 \text{ yr}$), but the multimonth HESS data no more indicate source variability *within* the observing period than the previous observations (Aharonian et al. 2004).

Intriguingly, the HESS data are also difficult to reconcile with the EGRET GC data (again, see Figs. 1 and 2 and also the inset of Fig. 4 of Aharonian et al. 2004), if one assumes a single source. We discuss this issue further below. For the moment, however, we must clearly decide on which of the TeV data sets we should base our analysis. Certainly one telling point against the CANGAROO data, as noted above, is the unusually steep, GC source spectrum. Although we do not pretend to have any in-depth knowledge of the workings of the CANGAROO analysis, we do note that observations of intrinsically bright regions like the GC are, generically, affected by the problem that at lower energies putative events can be “bumped over” a detector’s threshold by noise, whereas at higher energies such a mechanism would not be expected to be working.¹⁰ A source spectrum, then, might be

¹⁰ One way around this potential problem is to employ a “padding” procedure in which artificial noise is fed into the data to account for the systematic brightness differences between on-source and background observations. This is at the cost of reducing the signal-to-noise ratio and, therefore, raising the threshold for observations, but without such a procedure the artificial steepening of a power law is difficult to avoid. Now, the VERITAS Collaboration, in its analysis of the Whipple data from sources located in bright regions, employs exactly the padding procedure described immediately above (S. Fegan 2004, private communication). However, to the best of our knowledge, the CANGAROO Collaboration does not use this procedure. For this reason we believe that the slopes of the CANGAROO data on the GC source are questionable.

made to seem steeper than in actuality by this preferential recording of lower energy events. Furthermore, although the HESS and Whipple data are somewhat at variance, they are certainly less in conflict than either result is with CANGAROO (again, see Fig. 4 of Aharonian et al. 2004), so they support each other in a qualified sense. For these reasons we focus on the HESS and Whipple results and, then noting both the greater detail and statistical weight in the former, we finally are drawn to the conclusion that we should leave only the HESS data in our analysis.

4.7. Other Neutron Production Channels in the GC Environment?

There are two channels other than p - p that might reasonably contribute to EHE neutron production at the GC that we mention in passing. These are p - γ and heavy-ion dissociation. Both of these operate, effectively, without producing a concomitant GeV or TeV gamma-ray signal. This has the implication that our calculation of EHE neutron production (normalized to this gamma-ray signal) is, all other things being equal, a strict underestimate.

4.7.1. p - γ Interactions

We have performed detailed calculations of the p - γ process within the $\Delta(1232)$ resonance approximation (Stecker 1979; Mucke et al. 1999; Dermer 2002). In this context, the relevant neutron production channel is through the first Δ resonance at 1232 GeV,

$$p\gamma \rightarrow \Delta \rightarrow n\pi^+, \quad (25)$$

with a cross section of about 6×10^{-28} cm² (Hagiwara et al. 2002). Here the branching ratios of the $\Delta(1232)$ lead to proton to neutron production in the well-defined ratio of 2:1 and its decay kinematics predicts a nucleon elasticity of 0.8 (Mucke et al. 1999). The interaction can take place if the energy of the ambient photon in the p rest frame, $E_{\gamma(p)}^{\text{thresh(pion)}}$, satisfies

$$E_{\gamma(p)}^{\text{thresh(pion)}} \geq \frac{m_{\Delta}^2 - m_p^2}{2m_p} \simeq 340 \text{ MeV}. \quad (26)$$

This means that the relevant target photon population in the GC context is supplied by the intense flux of IR photons from the circumnuclear disk. This is a powerful source ($\simeq 10^7 L_{\odot}$) of reprocessed mid- to far-infrared continuum emission with a dust temperature of $\simeq 100$ K (Telesco et al. 1996). Given this temperature, we find that the p - γ process does not contribute significantly for neutron production until proton energies of $\geq 6.9 \times 10^{18}$ eV are reached or, given the elasticity, does not contribute significantly to neutrons with energies below $\sim 5.5 \times 10^{18}$ eV. (The fact that this reaction does not “kick in” until such high energies explains why it cannot be directly normalized to the GeV gamma-ray signal: despite the fact that the decay of neutral pions from the other branch of the Δ decay will certainly produce photons, these will all be directly produced in the EHE regime.) This fact, as our detailed modeling shows, means that the p - γ process produces an EHE neutron flux in the relevant energy range, at most, $\mathcal{O}(1\%)$ of that due to p - p and may, therefore, be ignored.

Note that we have performed the calculations in this section assuming that the interaction region is at parsec scales from the GC (appropriate, e.g., to the closer-in parts of the Sgr A East

shell). We explain in § 6.1 why it is unlikely that the interaction region is very much closer to the GC than this.

4.7.2. Heavy-Ion Dissociation

A calculation of neutron production from dissociation of heavy ions (through interactions with either ambient protons or light) is beyond the scope of this paper (Tkaczyk 1994). Such interactions, moreover, do not lead directly to photon production at any energy and we cannot, therefore, normalize the rate of this process to the EGRET gamma-ray data directly. Still, that this mechanism might be operating we find entirely plausible, especially given the fact that heavy ions make up a non-negligible fraction of the detected CR population.

5. FITTING TO ALL DATA

We now attempt to derive a best fit to the following data: the EGRET gamma-ray differential flux at \sim GeV energies, the HESS \sim TeV gamma-ray flux, and the EHE ($\sim 10^{18}$ eV) CR anisotropy data (assumed to be due to neutrons). Such a fitting procedure makes sense in principle because, as shown above, the neutron and photon fluxes are governed by power laws with the same spectral index (as both these species arise from the interactions of the same parent spectrum of accelerated protons) and at any energy we can relate the flux or differential flux of neutrons and photons.

Our procedure is to define a χ^2 function that depends on the differences between fitted and observed fluxes or differential fluxes, weighted by the experimental error in each flux measurement and also allowing for the systematic uncertainty in the energy calibration of the various instruments. The free parameters in our analysis are the spectral index, γ , and the normalization of the gamma-ray differential flux.

Employing this procedure, one quickly learns that the hypothesis that the totality of gamma-ray and CR data can be explained as arising from the interactions of a single, parent population of shock-accelerated protons is not supported by the data: the fit procedure produces a χ^2 of 78.55 with a reduced χ^2 of 6.54 for the $14 - 2 = 12$ degrees of freedom (dof), which is a very bad fit. There are a number of caveats to this bald assertion, however, which we explore in somewhat greater detail below. These are, first, that it assumes that the detected radiation, in its various energy regimes, is all equally unaffected in its propagation. A process that, for example, attenuated gamma rays at TeV energies but not at GeV energies might be operating, but this is not accounted for in the fitting procedure. Second, the fits assume that there is, effectively, only a single source. The GC is a highly energetic and dense region; there could then, in reality, be a number of effective sources or acceleration/interaction regions (characterized by different magnetic field strengths, different shock compression ratios, different shock/magnetic field geometries, different ambient particle densities, etc.) there. Third, the fit procedure assumes that the detected particles/radiation all originate in the same p - p collision process. If, say, another process were operating at high energies to supply some significant fraction of the observed neutrons, then accounting for this process might allow for a better fit to the totality of data (that said, the EGRET and HESS data are still difficult to reconcile). We now explore these various points in greater detail.

5.1. A Single Source: Attenuation of TeV Photons?

As should be expected from § 4.5, if one performs a fit to only the EGRET+EHECR data (“EHECR” denotes extremely high energy CR: it is implicit in our analysis, of course, that these data

are explained as arising from neutron primaries), neglecting the HESS data, one finds a very good fit: the total χ^2 is 0.33 for $4 - 2 = 2$ dof for a very plausible spectral index of 2.23. We remind the reader that this value is perfectly consistent with that determined by Fatuzzo & Melia (2003) for the EGRET source 3EG J1746–2851 and by Bossa et al. (2003) for the EHE CR source seen by AGASA (both these references quote a figure of 2.2) and is, moreover, perfectly consonant with the expectation from theory for acceleration at strong shocks. Further, the fitting points are around 9 orders of magnitude apart, so it is, indeed, remarkable that the fit obtained between such widely separated data points should require a spectral index so close to the expectation from shock acceleration theory and previous observations in more limited energy regimes (see the upper line in Fig. 1).

The one problem with this scenario is the significant (by a factor of ~ 20) overprediction of TeV gamma rays (again, see Fig. 1). We note that there is no question that our fit to the EGRET+EHECR data does predict a TeV source that is inside the field of view of HESS’s GC observations (and Whipple’s for that matter) and should have been seen by this instrument. The simplest possibility to resolve the discrepancy, which we respectfully submit, is that the normalization of HESS GC data is simply off by a large number. In support of this, note that the other remarkable aspect of Figure 1 is that the lower line, which is a fit to the 2003 July–August HESS data alone, so closely parallels the upper: it has a best-fit spectral index of 2.22.¹¹ It does seem rather unlikely, however, that a normalization error could really be as large as we require it, and, given also that even the larger Whipple flux determination is still deficient with respect to our expectation from the single source model, we are compelled to seek astrophysical explanations of the data considering them to be fundamentally sound.

One possibility, presaged above, is that some process is acting to attenuate or downgrade the energies of the \sim TeV photons *after* they have been generated, i.e., in their propagation from interaction point to us. In this regard, probably the most attractive mechanism is pair production on the optical–NIR background near the source. Certainly something like this process is known to operate in the “self-absorption” of TeV gamma rays from some X-ray binary systems by the thermal photons emitted by those systems’ own accretion disks (for a review see Moskalenko 1995). Pair production has an effective threshold, which means that it does not significantly attenuate gamma rays with energies below a threshold, $E_{\gamma}^{\text{thresh(pair)}}$, given roughly by

$$E_{\gamma}^{\text{thresh(pair)}} \sim 1 \left(\frac{E_{\text{bgnd}}}{0.5 \text{ eV}} \right)^{-1} \text{ TeV}, \quad (27)$$

where E_{bgnd} is the typical energy of the (relevant) background photon population. With NIR–optical background light, then, the GC GeV signal would remain unattenuated as desired. From equation (27) we require a background of ~ 1.5 eV (i.e., NIR–optical) photons to attenuate the HESS signal right down to the lowest datum at around 300 GeV. Further considerations are the following:

1. Attenuation of the signal by $\sim 1/20$ of the expectation (given the fit to the other data) implies an optical depth of $\ln(20) \sim 3$.

¹¹ This spectral index has been independently rederived by us: the HESS group finds a spectral index of 2.21 ± 0.09 with a normalization of $2.5 \times 10^{-8} \text{ m}^{-2} \text{ s}^{-1} \text{ TeV}^{-1}$ at 1 TeV. We perfectly agree with this normalization to the limit of the significant figures quoted.

2. The peak cross section for pair production is roughly 10^{-25} cm^2 , so we require a column density of photons of around $3/10^{-25} \text{ cm}^2 = 3 \times 10^{25} \text{ cm}^2$ to attenuate the photons. Over the entire 8.5 kpc to the GC this would require an average optical–NIR photon number density of $\sim 1000 \text{ cm}^3$. This is orders of magnitude larger than what is found in the Galactic plane, so we concentrate on the idea that most attenuation will happen very close to the GC source.

3. Given the similarities in the slopes of the fitted power laws shown in Figure 1, the attenuation/degradation should be energy independent over the observed TeV data points. At the heuristic level, at least, pair production can achieve something like this (although this is somewhat dependent on the distribution of the target photon population) once one accounts for the possibility that the daughter electron-positron pairs go on to produce further, high-energy gamma rays by inverse Compton scattering of light in the background radiation field, thereby initiating a cascading process that redistributes the photon energy.¹²

4. The main remaining question now is simply whether we can plausibly get a sufficient column density of NIR–optical photons near a candidate GC source to affect the attenuation/degradation. For reasons that are explained in § 6 the two objects we consider plausible sources for the EHE CRs are the accretion disk associated with the GC black hole itself, Sgr A*, and an SNR located very close to the GC called Sgr A East. We consider the photon environments in the immediate vicinity of each of these before briefly considering the general, GC photon number density (i.e., within ~ 10 pc of the center):

*Sgr A**.—Genzel et al. (2003) find that the “local background-subtracted” luminosity of Sgr A* in the NIR is $\sim 3.8 \times 10^{34} \text{ ergs s}^{-1}$. This means that, assuming a point source, a column density along a radial direction starting at r_0 is given by $2.7 \times 10^{34} (r_0/\text{cm})^{-1} \text{ cm}^2$. Setting this equal to the required column density ($3 \times 10^{25} \text{ cm}^2$) and inverting, we find $r_0 \sim 10^9 \text{ cm}$. However, this is inside the Schwarzschild radius of the central black hole ($\sim 8 \times 10^{11} \text{ cm}$) and, therefore, an unphysical requirement. The NIR light field due to the Sgr A* accretion disk, in other words, cannot attenuate the TeV gamma rays to the extent we require. We note in passing that postulating a source location very close to the central black hole would present many observational difficulties. These are summarized in § 6.1.

Sgr A East.—From Figure 3 of Melia et al. (1998) the extrapolated synchrotron flux at ~ 1 eV for this object is $0.3 \text{ MeV cm}^{-2} \text{ s}^{-1} \text{ MeV}^{-1}$. This translates to a rough (number) luminosity of $2.6 \times 10^{45} \text{ photons s}^{-1}$, which is an order of magnitude smaller than that for Sgr A*, which means an analogous r_0 many orders of magnitude too small given the \sim pc scales of the Sgr A East shock(s).

General background.—On the other hand, the actual quantity of interest is not the background-subtracted luminosity or the luminosity due to any particular object. Rather, it is the total number density of suitable photon targets in the GC environment. This we can estimate from the following consideration: Wolfire et al. (1990) find that the GC circumnuclear disk requires an ionizing UV photon flux of $100\text{--}1000 \text{ ergs cm}^{-2} \text{ s}^{-1}$. Taking the upper figure and assuming the same energy density in NIR

¹² In this regard, consider Figs. 6a and 6b of Carraminana (1992), which show the results of detailed modeling of the “self-attenuation” of TeV gamma rays from two X-ray binary systems due to interactions with thermal NIR and optical photons emitted by those systems’ own accretion disks. It can be seen in these figures that the resultant (downshifted) spectrum parallels the unmodified spectrum for up to an order of magnitude in energy.

photons,¹³ one finds (at ~ 1 eV) a photon number density of $2.1 \times 10^4 \text{ cm}^{-3}$. Again, given the specified column density, this number density requires a length scale of $1.5 \times 10^{21} \text{ cm} \sim 500 \text{ pc}$ to get sufficient attenuation. This would seem to be excessive.

We reluctantly conclude, then, that around neither of the plausible, GC sources of the EHE CRs, nor in the general GC environment, does one find a large enough NIR–optical photon number density (over sufficient scales) for our purposes: the optical depth to pair production experienced by the TeV gamma rays in their propagation out of the GC environment is too small for us to explain the totality of data with a single source. We now therefore consider the idea that two effective sources are contributing to the totality of data, with one source explaining the EGRET results and another (we hope) able to account for both the HESS and EHE CR observations. In this scenario we do not have a compelling explanation for the closely parallel nature of the two fitted lines in Figure 1 aside from the general expectation from shock acceleration theory that the spectral index be close to 2.0 in a strong shock.

5.2. Two Effective Sources?

In introducing the idea that there may be two *effective*¹⁴ sources, we note that this is not an entirely unnatural reading of the situation. There are two pieces of evidence we bring in here:

1. It has actually been determined by Hooper & Dingus (2002) in their reanalysis of select data from the 3EG catalog (Hartman et al. 1999) that the true GC is excluded at the 99.9% confidence limit as the true position of the source 3EG J1746–2851 (this determination is at variance with the findings made in Hartman et al. 1999). Hooper & Dingus (2002) found the EGRET maximum likelihood source position, at the 50% confidence level, to lie at a position $0^{\circ}21$ from the GC (i.e., $\sim 30 \text{ pc}$ at this distance), but with the higher confidence level regions for source position (68%, 95%, and 99%) noticeably smeared in toward the GC. In contrast, the HESS GC source was found to lie with 95% confidence within $0^{\circ}05$ of the GC (Aharonian et al. 2004).

2. Both modeling and observation of SNRs over many years have consistently shown that those examples with high flux tend to have a lower energy cutoff than those whose spectrum extends to higher energies. This is generally attributed to the fact that physical conditions that sponsor efficient acceleration also lead to efficient cooling at higher energy. In general, then, the flux level and energy cutoff tend to go in opposite directions (see, e.g., Baring et al. 1999).

On the quantitative side, the first item we must now check is whether a good fit is possible to the combined HESS+EHECR data, which, in this scenario, are supposed to be explained by a single source (we call this assumed high-energy source the “HE source”). We find this, indeed, to be the case: such a fit produces a χ^2 value of 4.6 and a reduced χ^2 of 0.51 for $11 - 2 = 9$ dof. The best-fit spectral index is very hard: 1.97. If we constrain the spectral index to be 2.0 and fit only to the normalization, we

obtain a χ^2 of 5.0 and a reduced χ^2 of 0.50 for $11 - 1 = 10$ dof (see Fig. 2).

The second issue we must confront is whether the other source (which we label the “LE source”), associated with the signal seen by EGRET, in any way interferes with the TeV observations that are ascribed to the HE source. In particular, we must determine whether the LE source is “overtaken” by the HE source at or below HESS energies as we require (in order that \sim TeV gamma rays not be overproduced). This might happen in either (or in an effective combination of) two ways: (1) if the spectral slope of the LE source is sufficiently steeper than the HE source and/or (2) if the LE source cuts out below TeV energies (the requirement that this source not produce a relatively significant flux of 300 GeV and above gamma rays would be guaranteed if the parent protons cut out at or below \sim TeV).

In regard to cases 1 and 2 immediately above, we note first that case 1 appears not to be the case: we have tried two approaches here and both *overpredict* the differential gamma-ray fluxes at \sim TeV by at least an order of magnitude. In the first approach we fit only to the three (highest energy) EGRET data points for 3EG J1746–2851 with variable normalization and spectral index. This naive approach produces a very steep spectral index of 2.6. In the second approach we fit only to normalization fixing the spectral index to 2.4, which is at the upper limit of the spectral index range for the parent proton spectrum as determined by Fatuzzo & Melia (2003) in their fit to the totality of the EGRET data (i.e., all nine data points). We should consider, then, whether case 2 could describe the situation.

The interesting question now is, therefore, how we arrange for the difference of something like 7 orders of magnitude between the maximum energies attained in the LE and HE GC sources. Certainly variation in ambient particle densities and magnetic field strengths will go some way toward explaining the difference, but it is doubtful that the combination of these two could give a difference of 10^7 . Another tenable hypothesis is that the LE source, which in this scenario would be entirely independent of the HE source, has an age-limited maximum energy. Another scenario would posit that the lion’s share of the difference may be attributed to differences in shock geometries. In particular, one could postulate that the HE source realize a perpendicular shock configuration and that the LE source be described by a parallel configuration. This difference would be expected to contribute to at least 2 orders of magnitude variation in maximum acceleration energies (all other considerations aside; see the Appendix, in particular, eqs. [A4] and [A7]). Note that we would also expect different shock compression ratios in the different effective sources so the generic expectation would be for differing spectral indices.

6. IDENTIFYING THE GC NEUTRON SOURCE

We now discuss the astrophysical objects located in the GC region that are credible candidates for the source of the various observed high-energy signals. Basically two objects stand out a priori: the accretion disk associated with the supermassive black hole at the Galactic dynamical center, Sgr A*, and the unusual, GC region SNR Sgr A East. As we discuss, however, various theoretical and observational considerations finally favor the latter object as the likely source.

6.1. Sgr A* as EHE GC Neutron Source

The question of the maximum energy to which protons might be accelerated at the Sgr A* shock has been addressed at some

¹³ A reprocessed IR photon background of similar energy density to the 30,000 K UV background is, in fact, expected, but this would realistically peak at around 100 K $\sim 2.3 \times 10^{-2}$ eV (see § 4.7.1). Given that, in any case, we do not find any positive effect from the reprocessed IR photons, this detail need not concern us.

¹⁴ We emphasize “effective” here because two or more apparent sources might in fact originate from a background population of protons accelerated in different regions of a single, extended object.

length by Markoff et al. (1999), and here we simply quote their results. As presaged above, these authors found that p - p collisions are the dominant energy loss process for relativistic protons: p - γ processes are suppressed relative to the expectation from other galactic nuclei owing to the very low luminosity of the GC, and p - e^- processes are also suppressed owing to a dearth of extremely energetic electrons. Taking the mass of the central black hole to be $(2.61 \pm 0.65) \times 10^6 M_\odot$ (Eckart & Genzel 1997),¹⁵ the shock to be located at 40 Schwarzschild radii, a (generously large) magnetic field of $\simeq 300$ G, and, finally, an ambient proton density of $\simeq 2 \times 10^8 \text{ cm}^{-3}$, Markoff et al. (1999) determine that the maximum attainable Lorentz factor for relativistic protons is approximately 4×10^8 , which translates to $E_p^{\text{max}} \simeq 4 \times 10^{17}$ eV. This maximum energy, then, means that Sgr A* is probably not the source of the putative EHE neutrons seen by AGASA and SUGAR (indeed, even if the anisotropy is due to the direct interactions of the primary, accelerated protons, it still cannot be the source).

Another factor supporting the view that Sgr A* cannot be the source of the observed EeV neutron flux would be the inconsistency implied by the emissivity of secondary particles. The ensuing particle cascade would produce a copious supply of energetic electrons and positrons that, in the presence of the inferred ~ 1 – 10 G magnetic field (let alone the 300 G field we used for the estimate above) for this source, would greatly exceed Sgr A*'s observed radio flux. This problem is alleviated if instead the secondary particles gyrate in the much weaker field associated with a typical supernova shell. Finally, Kosack et al. (2004) make the point that the lack of variability seen in their \sim TeV gamma-ray data for the GC source is evidence against the identification of this source with a compact point source such as Sgr A* (no evidence for variability is seen in the EGRET data for 3EG J1746–2851 either; Mayer-Hasselwander et al. 1998).

6.2. Sgr A East as EHE GC Neutron Source

6.2.1. Introduction to Sgr A East

Sgr A East is a mixed-morphology, $\mathcal{O}(10^4)$ year old SNR located within several parsecs of the GC (see Melia & Falcke 2001). It appears to be of the class of SNRs that have been observed and detected at 1720 MHz (the transition energy of OH maser emission), such emission being a signature of shocks produced at the interface between supersonic outflow and the dense molecular cloud environments with which these SNRs are known to be interacting. There is, further, good evidence (see below) that Sgr A East may be associated with the EGRET source 3EG J1746–2851 introduced in § 4.2. It should be remarked, however, that if this putative association is real, Sgr A East has a gamma-ray luminosity ($\sim 2 \times 10^{37}$ ergs s^{-1}) almost 2 orders of magnitude greater than that of the other EGRET-detected SNRs, something that clearly demands explanation.

In fact, in a self-consistent scenario explored elsewhere (Melia et al. 1998; Fatuzzo & Melia 2003) the Sgr A East remnant has been shown to be capable of producing the observed gamma-ray luminosity once the unusually high ambient particle density ($\gtrsim 10^3 \text{ cm}^{-3}$) and strong magnetic field ($\gtrsim 0.1$ – 0.2 mG) at the GC are taken into account. Indeed, let us make the natural assumption that there is a population of protons at Sgr A East

accelerated by the shocks associated with the supernova blast wave (and, therefore, governed by a power law with spectral index ~ 2). Then, from collisions between these high-energy protons and ambient ions, pions will be produced and these will, in turn, decay to produce photons. Now, the high-energy gamma-ray luminosity in this scenario is essentially dependent on the rate of collisions between ambient ions and high-energy protons, which is, in turn, dependent on the product of the ambient ion density and the high-energy proton density, $n_H n_0$. Thus, we can fit to these two on the basis of the observed gamma-ray spectrum. However, we also have a handle on n_H from observations by ACIS on board *Chandra*: Sgr A East is expanding into an ionized gas halo with a density $\sim 10^3 \text{ cm}^{-3}$ and interacting with a cloud of density $\sim 10^5 \text{ cm}^{-3}$ (Maeda et al. 2002). Further, the total energy in the accelerated proton population is readily calculated from n_0 and is, of course, constrained to be less than the total energy released in the original explosion that gave birth to the Sgr A East shell.

These considerations result in fairly rigorous constraints on any attempted fit to observations of Sgr A East. But with a proper treatment of pion production (in particular, the energy dependence of the pion multiplicity), the entire broadband spectrum of the object can be compellingly explained. This explanation essentially sees the super-100 MeV gamma-ray spectrum as due to π^0 decay, the sub-100 MeV gamma-ray spectrum explained by bremsstrahlung emission (self-consistently with the assumed value for n_H , namely, 10^3 cm^{-3} ; see below), and the VLA¹⁶ observations of Sgr A East at 6 and 20 cm explained by synchrotron emission (although see below for a caveat regarding the radio spectrum). Note that in this scenario it is the secondary, charged leptons (ultimately resulting from collisions of the shock-accelerated protons with ambient ions) that are responsible for the bremsstrahlung and synchrotron emission, rather than directly accelerated leptons. Indeed, the population of this primary lepton class can, in fact, be shown to be negligible in comparison with the secondaries, given that each accelerated proton produces of order 20–30 charged leptons (Fatuzzo & Melia 2003).

In regard to Sgr A East's radio spectrum, it should be noted that the synchrotron emission from the total population of secondary, charged leptons is not *directly* consistent with radio observations: the observed spectral index is ~ 1 , pointing to an underlying population of nonthermal charged leptons with a power-law distribution of index ~ 3 (Pedlar et al. 1989). In contrast, from general considerations (whether the lepton population is directly accelerated or born of the interactions of shock-accelerated protons), we expect the lepton index to be ~ 2 , leading to radio emission characterized by a spectral index ~ 0.5 . If, however, one allows for the reasonable eventuality that high-energy leptons diffuse out of the Sgr A East region, the convolution of a diffusion loss factor with the initial lepton spectrum resulting from pion decay allows a very good fit to the radio spectrum (Fatuzzo & Melia 2003). Alternatively, it might be that the high-energy protons themselves are diffusing out of the system, thus also (indirectly) depleting the high-energy lepton spectrum. This scenario also provides a credible, although less good, fit to the radio data. As will become clear, however, the very fact that we do see a GC EHE CR anisotropy argues against the latter scenario.

¹⁵ Note that a recent revision to the Galactic center black hole mass that determines it to be $4.1 \pm 0.6 M_\odot$ (Ghez et al. 2003) does not substantially alter the conclusion of Markoff et al. (1999) regarding maximum attainable energies for shocked protons.

¹⁶ The National Radio Astronomy Observatory is a facility of the National Science Foundation operated under cooperative agreement by Associated Universities, Inc.

The scenario presented above, which we label “HIGH,” is to be contrasted with an alternative picture (“LOW”) explored earlier (Melia et al. 1998), in which a considerably lower ambient particle density was employed (viz., $\sim 10 \text{ cm}^{-3}$). Through the $n_{\text{H}}n_0$ dependence of the gamma-ray luminosity, this then necessitated a large population of high-energy protons, in turn yielding an energy content of relativistic particles of $\sim 8 \times 10^{50}$ ergs. In contrast, the particle energy calculated for the HIGH scenario is $\sim 10^{49}$ ergs, so clearly the view that Sgr A East resulted from a standard supernova favors HIGH. Moreover, the recent *Chandra* observations of Sgr A East alluded to above support the view that Sgr A East is, indeed, the remnant of a single supernova with typical energetics.

6.2.2. Ambient Magnetic Field at Sgr A East

The first input we require to determine the maximum energy of protons accelerated in the Sgr A East shock is the ambient magnetic field strength. Typically, the magnetic field strength in the interstellar medium scales as the square root of the density. In the case of Sgr A East, it appears that most of the p - p scatterings (and essentially all of the bremsstrahlung and synchrotron emissivity) occur in the $\sim 10^3 \text{ cm}^{-3}$ region, where the field strength is ~ 0.2 mG. Thus, if the shock occurs in the $\sim 10^5 \text{ cm}^{-3}$ molecular cloud colliding with the expanding shell, the field intensity within the particle acceleration region may be as high as a few milligauss. Note that the latter field strength is entirely consistent with that determined directly from polarimeter observation of the general GC region (Chuss et al. 2003).

6.2.3. Maximum Energy of Protons Accelerated by the Sgr A East Shock

With a field strength of 4 mG, the other inputs described above, and the application of equation (A7) from the Appendix, one finds that particles in the Sgr A East shock can be accelerated, in principle, to $10^{19} R_{\text{shock}}/(10 \text{ pc})Z$ eV assuming that a perpendicular shock configuration is realized. This figure is not limited by cooling or age considerations: from equation (A10) we find that, given the assumed 3000 cm^{-3} ambient proton density,¹⁷ a lower limit on the cooling-limited maximum energy is $\eta 2.7 \times 10^{21}$ eV (this is a lower limit because it has been derived assuming a p - p cross section of 150 mbarn, which, in fact, only pertains at the very highest region of the pertinent energy range). Moreover, the time required by the 4 mG field to accelerate protons to this energy is around 2500 yr, comfortably inside the $O(10^4)$ year age of the remnant (the age-limited energy using eq. [A11] is around $\eta 5 \times 10^{20}$ eV for a 4 mG field and an age of 10,000 yr).

Parentetically, note from the above that heavier ions might be accelerated to energies approaching 10^{20} at Sgr A East, potentially explaining most of the CR spectrum even above the ankle. If this were the case, it would *not* imply an unambiguous anisotropy toward the GC: even at 10^{19} eV modeling shows that a proton leaving the vicinity of the GC would be scattered many times, on average, before it could reach us at Earth. This mechanism would isotropize the GC signal even at these extreme energies, although they would probably not completely wash it out. Such a scenario is not ruled out by current observations.

6.2.4. Sgr A East and the Two-Source Model

We note finally that there being two effective sources required to explain the totality of data fits naturally into the hypothesis that the Sgr A East shell accelerates all the protons required to explain the various signals. The Sgr A East shell ranges in distance from very close to the GC (within 1 pc) to up to ~ 10 pc. It subtends, therefore, regions of widely varying ambient particle density and also magnetic field strength and orientation so that proton populations accelerated in it would be expected to display or experience varying maximum energies, spectral indices, and overall (energy) differential number densities and interaction rates. Moreover, the aforementioned determination by Hooper & Dingus (2002) that the EGRET source center of gravity is 0.21 (i.e., ~ 30 pc) away from the actual GC (while the HESS source’s center of gravity is localized to *within* $1'$ or ~ 2.5 pc of the GC) supports this basic idea: the lower energy source is located in a region where ambient magnetic fields can be expected to be lower and also, perhaps, where ambient particle densities can be expected to be higher, whereas the higher energy source is located in a region of larger magnetic field strength. We hypothesize also that the acceleration in these regions be described by different shock/magnetic field geometries (with the EGRET source describing a parallel shock–magnetic field configuration and the HESS/CR source being described by the more efficiently accelerating perpendicular configuration). Further observations and modeling will be required to determine whether this picture is tenable.

7. CONCLUSIONS

We have examined, and shown to be quantitatively successful, the idea that the Galactic center EGRET source 3EG J1746–2851 is also responsible for the observed anisotropy that is seen in CRs toward the GC at an energy of around 10^{18} eV. We have, in particular, demonstrated that a power-law fit to the \sim GeV EGRET data and the EHE CR anisotropy data (taking the latter to be evidence for neutron primary particles) requires a parent proton population with a spectral index of 2.23. This is in exact agreement with previous determinations made (individually) for the spectral indices of the parent proton population that is generating the EGRET-observed gamma rays and for the distribution of the EHE CR signal. The determined spectral index is also in perfect agreement with the expectation from shock acceleration theory. Our fitting procedure requires input from the particle physics of charge exchange in p - p collisions. Our results imply the existence of a population of shock-accelerated protons (and perhaps heavier ions) at the GC with energies that range up to, at least, $\sim 10^{19}$ eV.

Unfortunately, however, this fit overpredicts the flux of gamma rays from the GC at \sim TeV energies given the existing data from a number of atmospheric Cerenkov telescopes (which are, admittedly, somewhat at variance among themselves). We show that what we believe to be the best and most recent data, those coming from the HESS instrument, are well fitted by a power law with a spectral index of 2.22, i.e., very close to the power-law fit to the combined EGRET and EHE CR data. One explanation, then, of the deficiency of the \sim TeV data with respect to expectation is that the HESS instrument’s normalization is wrong by a large (energy independent) factor (~ 20). Finding this somewhat unlikely, however, we have sought astrophysical explanations of the totality of EGRET+HESS+EHECR data, taking these all to be fundamentally sound. Pursuing the idea that all the data might be explained as originating from the interactions of a single high-energy proton population, we searched

¹⁷ As is the case at Sgr A*, p - p collisions are the dominant cooling mechanism for relativistic protons accelerated at the Sgr A East shock (Melia et al. 1998; Fatuzzo & Melia 2003).

for mechanisms that would (preferentially) attenuate the \sim TeV gamma rays. The most promising candidate in this direction, however, viz., pair production on an assumed 1.5 eV light background, we have found is unlikely to be efficacious as the number density of such photons in and around candidate GC sources or source regions is probably too low.

Noting these facts, we sought for a model involving two effective sources. We showed here that the hypothesis that the EGRET data are explained by one source and the HESS+EHECR data by another is perfectly tenable with, in particular, a good fit possible to the combined HESS+EHECR data. This two-source scenario, which has some plausibility given the varying source position determinations made on the basis of observations conducted in the various energy regimes, requires that the EGRET source probably be steeper than (and certainly have a cutoff energy much lower than) the HESS+EHECR source.

This difference in maximum particle energies could be attributed to completely independent populations of high-energy protons, accelerated in different astrophysical sources with differing ages, magnetic field strengths, ambient particle densities, etc. Alternatively, and more plausibly in our opinion, a population of high-energy protons accelerated in different regions (with differing magnetic field/shock geometries) of a single, extended object might produce two (or more) effective sources.

We have shown that the Sgr A East SNR (located near the GC) could provide the environment in which the acceleration of the high-energy protons we require could plausibly be achieved. Further, we have shown that the two-source model fits naturally with the hypothesis that Sgr A East is the accelerated proton source: the Sgr A East shell ranges in distance from very close to the GC (within 1 pc) to up to 10 pc distance. It subtends, therefore, regions of widely varying ambient particle density and magnetic field strength and orientation so that proton populations accelerated in it would be expected to display or experience varying maximum energies, spectral indices, and overall (energy)

differential number densities and interaction rates. On the other hand, it seems that the other plausible GC source, namely, the accretion disk around the GC black hole, Sgr A*, is unlikely to provide an environment in which acceleration of protons to the extreme energies required is possible. Further, observations give evidence against a pointlike source for both the GeV and TeV regime gamma rays. Our results, then, provide tentative evidence for the first direct connection between a particular, Galactic object (Sgr A East) and the acceleration of CRs up to energies near the ankle in the CR spectrum.

At all energies, we anticipate, with great interest, the results that shall be obtained by the next generation of instruments. These instruments include the GLAST Large Area Telescope (Thompson 2004) at \sim GeV energies, VERITAS (Krennrich et al. 2004) at \sim TeV energies, and, finally, the Pierre Auger Observatory (Camin 2004) for CRs of 10^{18} eV and higher. The results from these instruments will either confirm or rule out our scenario.

R. M. C. gratefully acknowledges useful communications from Paolo Lipari and enlightening conversations with Matt Holman, Jasmina Lazendic, Avi Loeb, and Josh Winn. F. M. would like to thank Steve Fegan and Trevor Weekes for very helpful correspondence. This research was supported in part by NASA grant NAG5-9205 and NSF grant AST 04-02502 at the University of Arizona. R. R. V. and F. M. are also partially supported by a joint Linkage-International grant from the Australian Research Council. R. R. V. thanks Paolo Lipari and Todor Stanev for general discussions on CRs and the observed anisotropies, and he thanks Paolo Lipari and Maxim Khlopov for their kind hospitality at the Università di Roma “La Sapienza” where these discussions took place. M. F. is supported by the Hauck Foundation through Xavier University.

APPENDIX

LIMITING ENERGIES AT PARALLEL AND PERPENDICULAR SHOCKS

In determining the limiting energy at an astrophysical shock, E_p^{\max} , two broad considerations play a part, viz., (1) the *intrinsic* limits to E_p^{\max} given the macroscopic properties of the shock at the source doing the acceleration (magnetic field strength, shock size, geometry, age, etc.) and (2) limits to E_p from heating-cooling balance, which we label “scattering” limits.

We discuss cases 1 and 2 at greater length below.

A1. PERPENDICULAR SHOCK ACCELERATION

A1.1. Transport

The whole of diffusive shock acceleration theory can be obtained from the Parker equation, the fundamental transport equation for the charged particle distribution function, $f(\mathbf{r}, t, \mathbf{p})$, in a background, collisionless hydromagnetic field (Parker 1965). This equation describes the effects of diffusion, convection, and acceleration/deceleration by an electric field on the charged particle distribution. We can arrive at a completely general description of diffusive shock acceleration (i.e., applying equally well to parallel and perpendicular shocks and everything in between) by putting a step function U into the Parker equation. The equation assumes that (1) the diffusion approximation holds good, i.e., that particles are scattered often enough by magnetic field irregularities that the particle distribution is nearly isotropic, and (2) the ratio of the shock speed, $U = |U|$, to the particle speed, w , is small: $U/w \ll 1$. In this picture, particle acceleration is caused by two factors (Jokipii 1982, 1987):

1. The large relative motion between the (magnetic) scattering centers causing the diffusion (*a*) in front of the shock and (*b*) behind the shock.
2. Drift along the shock front (if the magnetic field has a component *normal* to the direction of propagation of the shock).

Despite the potential importance of the second factor listed above, many discussions neglect magnetic field changes and the resulting particle drifts, effectively restricting consideration to quasi-parallel shocks. The modification of the shock by the CRs may also be important (see, e.g., Jones & Kang 1992). However, this may not affect significantly the highest energies of interest here, as

their energy density is small. The following test particle calculation should give a reasonable approximation to the maximum energies.

A1.2. Acceleration Rate

In contrast to the spectral index, which, it can be shown, is universally close to 2.0 in all strong shocks, the high-energy cutoff of the accelerated particles *is* sensitive to the particulars of the shock. This maximum energy is largely determined by the time available to accelerate the particles and the rate of energy gain. These, in turn, are controlled by the finite lifetime of the shock itself, the escape of particles from the shock region, and the rate at which particles scatter back and forth across the shock (collision and synchrotron losses are also important, but these are dealt with below).

By solving the time-dependent Parker equation (and taking particles to be injected into the shock at t_0 with momentum p_0), we can determine that the particle distribution is governed by a universal power law with a high momentum cutoff, p_c , which satisfies

$$\frac{dp_c}{dt} \simeq U_{\text{shock}}^2 \frac{p_c}{4\kappa_{xx}}, \quad (\text{A1})$$

where κ_{xx} is the diffusion coefficient normal to the shock front. Either increasing the shock speed, U_{shock} , or decreasing the diffusion coefficient, therefore, will produce a greater rate of maximum momentum increase and, consequently, lead to faster particle acceleration in general. Now we can write the diffusion coefficient normal to the shock front as

$$\kappa_{xx} = \kappa_{\parallel} \cos^2(\theta_B) + \kappa_{\perp} \sin^2(\theta_B), \quad (\text{A2})$$

where θ_B is the angle between the shock normal and the magnetic field vector. One can see immediately, then, that if the shock is quasi-perpendicular, $\kappa_{xx} \simeq \kappa_{\perp}$, because κ_{\perp} is usually smaller than κ_{\parallel} , such a shock will tend to accelerate particles faster than a quasi-parallel shock.

Let us consider the two limiting cases, quasi-parallel and quasi-perpendicular shocks, in a little more detail.

A1.3. Limiting Energies in Quasi-Parallel Shocks

From equation (A1) together with the condition that λ_{\parallel} , the mean free path along the shock, must be of the order of or larger than the gyroradius of a particle at the limiting upper momentum, $r_g(p_c) \equiv r_c$, it may be determined that

$$\frac{1}{p_c} \frac{dp_c}{dt} \lesssim \frac{3U_{\text{shock}}^2}{4r_c w}. \quad (\text{A3})$$

This is the so-called Bohm limit on the acceleration rate. Many researchers have taken this to represent a mechanism-independent limit on the acceleration rate and, hence, indirectly on E_{max} . The logic implicit here is that in order to be turned about so that it recrosses the shock, a particle must be rescattered each time it moves upstream or downstream of the shock. The highest energy gain rate, by this logic, will then occur for the *smallest* scattering mean free path, which, in turn, cannot be smaller than the gyroradius. Using this result, together with the modified Sedov solution for U_{shock} , Lagage & Cesarsky (1983) determined that

$$E_{\text{max}}^{\text{SNR}} \sim E_{\text{max}}^{\text{LC}} \equiv \text{few} \times 10^{14} Z \text{ eV} \quad (\text{A4})$$

for the distance and magnetic field scales typical for a Galactic SNR (where Z denotes the charge of the particle or nucleus). Given that, as outlined above, SNRs are expected to accelerate the bulk of the CRs up to at least the knee at $\sim 5 \times 10^{15}$ eV, equation (A4) would seem to place a severe constraint on the mass composition of the CRs.

A1.4. Limiting Energies in Quasi-Perpendicular Shocks

The reasoning presented above does not have universal validity, however: if the magnetic field has a component perpendicular to the shock propagation direction and if (as is usually the case as mentioned above) $\kappa_{\parallel} > \kappa_{\perp}$ (so that the particle is less constrained in motion *along* the shock than in motion away from it), the gyromotion of a charged particle can carry it across the shock many times between each scattering. This can mean a much larger E_{max} than for the parallel case.

To see this quantitatively, note that the kinetic theory (i.e., billiard ball scattering) value for the ratio between perpendicular and parallel diffusion coefficients is given by

$$\frac{\kappa_{\perp}}{\kappa_{\parallel}} = \frac{1}{1 + (\lambda_{\parallel}/r_g)^2}, \quad (\text{A5})$$

so that for a larger parallel mean free path, the perpendicular diffusion coefficient is reduced and the acceleration is therefore increased (cf. the parallel case for which a smaller parallel mean free path means an increase in the acceleration rate). The billiard ball scattering result will change if more realistic turbulent magnetic irregularity scattering is used, but the essential result remains: the acceleration rate at a perpendicular shock can be much larger than at a parallel shock.

It seems that if we want acceleration to very high energies, we should simply dial up the required λ_{\parallel} . This quantity may not be increased without limit, however: there is a maximum value for λ_{\parallel} , which can be determined (interchangeably) by the logic that (1) the diffusion approximation implicit in the Parker equation ceases to be valid if particles do not scatter often enough to be isotropic at the

shock or (2) particles must scatter often enough to diffuse upstream fast enough to stay ahead of the shock (Jokipii 1982, 1987). Either of these two conditions leads to the requirement that for simple scattering

$$\Upsilon \simeq \frac{\lambda_{\parallel}}{r_g} \frac{U_{\text{shock}}}{w} \ll 1, \quad (\text{A6})$$

so that if $U_{\text{shock}}/w \ll 1$, then we can have $\lambda_{\parallel}/r_g \gg 1$ (while still maintaining eq. [A6]), giving us a significant enhancement over the Bohm acceleration rate.

This consideration is of immediate relevance to the SNR case: the sort of (globally) spherical shock produced by a supernova is quasi-perpendicular over much of its area, meaning that κ_{\perp} is much more important than κ_{\parallel} over a substantial fraction of the SNR shock. This means that $E_{\text{max}}^{\text{LC}}$ is actually a significant underestimate of $E_{\text{max}}^{\text{SNR}}$, which, by putting Υ equal to its maximum value, viz., ~ 0.3 , in equation (A6), we can determine to be

$$E_Z^{\text{max (perp)}} \sim 5 \times 10^{16} Z \left(\frac{B}{20 \mu\text{G}} \right) \left(\frac{R_{\text{shock}}}{10 \text{ pc}} \right) \text{ eV} \quad (\text{A7})$$

for a particle or nucleus of charge Z . Note that in the equation above ‘‘perp’’ signifies that the maximum energy appertains to acceleration in a perpendicular shock geometry (Jokipii 1982, 1987). This energy is amply large enough to accelerate CRs beyond the knee, but note that equation (A7) represents an in-principle limit: in general, cooling effects may more tightly limit the maximum energy/momentum to which the high-energy particle population can be accelerated. Further, the time available for acceleration is, of course, bound by the total age of the shock. We now discuss these additional constraints.

A2. COOLING- AND AGE-IMPOSED LIMITS TO MAXIMUM PARTICLE ENERGIES

There will, in general, be a maximum proton energy $E_p^{\text{max (cool)}}$ above which the combined energy loss rate due to many processes (proton synchrotron emission, inverse Compton scattering, and hadronic collisions [with ambient nucleons and photons]) will exceed the rate of energy gain due to shock acceleration.

Note that in the GC environment p - p collisions are, by far, the dominant energy loss process (Markoff et al. 1997; Melia et al. 1998; Fatuzzo & Melia 2003). This is the case because of the relatively lower density of target photons and the intrinsically smaller cross sections and inelasticities of p - γ processes in comparison with p - p collisions (this is to be contrasted with the situation that generally pertains in AGNs, where the photon density can be significantly higher than in the GC).

Thus, for the GC environment, $E_p^{\text{max (cool)}}$ depends on the functional form of the average p - p collision inelasticity, where inelasticity denotes the fractional energy loss in the collision (i.e., the energy of the leading baryon in units of the energy of the incoming proton). The timescale for proton cooling via p - p collisions is given by

$$t_{pp} \simeq \frac{1}{n_p c \sigma_{pp} K_{pp}}, \quad (\text{A8})$$

where the proton-proton cross section, σ_{pp} , and the fractional energy loss per p - p collision or *inelasticity*, K_{pp} , are both, in principle, dependent on energy.

On the other hand, the proton (shock) acceleration timescale is given by (Begelman et al. 1990)

$$t_p^{\text{acc}}(E_p) = \frac{E_p}{\eta c^2 e B}, \quad (\text{A9})$$

where η is a dimensionless parameter, $\mathcal{O}(1)$, that depends on the details of the acceleration mechanism.

We can determine E_p^{max} by setting $t_{pp} = t_p^{\text{acc}}(E_p^{\text{max}})$ and inverting to find

$$E_p^{\text{max (cool)}} \sim \frac{c \eta e B}{n_p \sigma_{pp} K_{pp}}. \quad (\text{A10})$$

Finally, in regard to maximum energies, one must also check that the timescale implied by equation (A9) for the maximum energy calculated using equation (A10) does not exceed the age, t_{age} , of the pertinent astrophysical object or environment. If this is the case, the maximum energy will be age limited, i.e.,

$$E_p^{\text{max (time)}} = \eta c^2 e B t_{\text{age}} \simeq 2.4 \times 10^{18} \left(\frac{B}{20 \mu\text{G}} \right) \left(\frac{t_{\text{age}}}{2.0 \times 10^4 \text{ yr}} \right) \text{ eV}. \quad (\text{A11})$$

In general we have, then,

$$E_p^{\text{max}} = \min \left\{ E_p^{\text{max (perp)}}, E_p^{\text{max (cool)}}, E_p^{\text{max (time)}} \right\}, \quad (\text{A12})$$

where the maximum energies are given, respectively, by equations (A7), (A10), and (A11).

REFERENCES

- Aharonian, F. A., et al. 2002, *A&A*, 395, 803
 ———. 2004, *A&A*, 425, L13
 Alvarez-Muñiz, J., & Halzen, F. 2002, *ApJ*, 576, L33
 Anchordoqui, L. A., et al. 2004, *Phys. Lett. B*, 593, 42
 Baring, M. G., et al. 1999, *ApJ*, 513, 311
 Bednarek, W., Giller, M., & Zielinska, M. 2002, *J. Phys. G*, 28, 2283
 Begelman, M. C., Rudak, B., & Sikora, M. 1990, *ApJ*, 362, 38
 Bellido, J. A., et al. 2001, *Astropart. Phys.*, 15, 167
 Biermann, P. L., et al. 2004, *ApJ*, 604, L29
 Bird, D. J., et al. 1999, *ApJ*, 511, 739
 Blasi, P., & Colafrancesco, S. 1999, *Astropart. Phys.*, 12, 169
 Blasi, P., & Melia, F. 2003, *MNRAS*, submitted
 Blobel, V., Fesefeldt, H., Franz, H., Geist, W. M., von Holt, K., Idschock, U., & Schmitz, N. 1978, *Nucl. Phys. B*, 135, 379
 Bossa, M., Mollerach, S., & Roulet, E. 2003, *J. Phys. G*, 29, 1409
 Camin, D. V. 2004, *Nucl. Instrum. Methods Phys. Res. A*, 518, 172
 Candia, J., Epele, L. N., & Roulet, E. 2002a, *Astropart. Phys.*, 17, 23
 Candia, J., Mollerach, S., & Roulet, E. 2002b, *J. High Energy Phys.*, 12, 32
 Capdevielle, J. N., & Attallah, R. 1992, in *AIP Conf. Proc.* 276, *Very High Energy Cosmic Ray Interactions*, ed. L. Jones (Melville: AIP), 448
 Capdevielle, J. N., Attallah, R., & Gabinski, P. 1992, in *AIP Conf. Proc.* 276, *Very High Energy Cosmic Ray Interactions*, ed. L. Jones (Melville: AIP), 442
 Carraminana, A. 1992, *A&A*, 264, 127
 Chilingarian, A., Martirosian, H., & Gharagyozyan, G. 2003, *ApJ*, 597, L129
 Chuss, D. T., et al. 2003, *ApJ*, 599, 1116
 Clay, R. W., et al. 2000, *Astropart. Phys.*, 12, 249
 Cline, D. B. 1988, in *Proc. RAND Workshop on Antiproton Science and Technology*, ed. B. Augenstein (New Jersey: World Scientific), 45
 Crocker, R. M., Melia, F., & Volkas, R. R. 2000, *ApJS*, 130, 339
 ———. 2002, *ApJS*, 141, 147
 Dao, F. T., et al. 1974, *Phys. Rev. D*, 10, 3588
 Dermer, C. D. 2002, *ApJ*, 574, 65
 Di Cocco, G., et al. 2004, preprint (astro-ph/0403676)
 Drury, L. O., Aharonian, F. A., & Voelk, H. J. 1994, *A&A*, 287, 959
 Eckart, A., & Genzel, R. 1997, *MNRAS*, 284, 576
 Engel, R. 2001, preprint (hep-ph/0111396)
 Engler, J., et al. 1975, *Nucl. Phys. B*, 84, 70
 Fatuzzo, M., & Melia, F. 2003, *ApJ*, 596, 1035
 Fatuzzo, M., Melia, F., & Rafelski, J. 2001, *ApJ*, 549, 293
 Flauger, W., & Mönning, F. 1976, *Nucl. Phys. B*, 109, 347
 Fleysher, R., et al. 2002, *BAAS*, 34, 676
 Forti, C., Bilokon, H., D'Ettore Piazzoli, B., Gaisser, T. K., Satta, L., & Stanev, T. 1990, *Phys. Rev. D*, 42, 3668
 Frichter, G. M., Gaisser, T. K., & Stanev, T. 1997, *Phys. Rev. D*, 56, 3135
 Gaisser, T. K. 1990, *Cosmic Rays and Particle Physics* (Cambridge: Cambridge Univ. Press)
 Genzel, R., et al. 2003, *Nature*, 425, 934
 Ghez, A. M., et al. 2003, *ApJ*, 586, L127
 Hagiwara, K., et al. 2002, *Phys. Rev. D*, 66, 010001
 Hartman, R. C., et al. 1999, *ApJS*, 123, 79
 Hayashida, N., et al. 1999a, *Astropart. Phys.*, 10, 303
 ———. 1999b, preprint (astro-ph/9906056)
 Hillas, A. M. 1980, in *Proc. 16th Int. Cosmic Ray Conf. (Kyoto)*, 6, 13
 Hinton, J. A. 2004, *NewA Rev.*, 48, 331
 Hooper, D., de la Calle Perez, I., Silk, J., Ferrer, F., & Sarkar, S. 2004, *J. Cosmol. Astropart. Phys.*, 9, 2
 Hooper, D., & Dingus, B. 2002, preprint (astro-ph/0212509)
 Huang, H. Z., et al. 2002, *J. Phys. G*, 28, 1667
 Jokipii, J. R. 1982, *ApJ*, 255, 716
 ———. 1987, *ApJ*, 313, 842
 Jokipii, J. R., & Morfill, G. 1991, in *Astrophysical Aspects of the Most Energetic Cosmic Rays*, ed. M. Nagano & F. Takahara (Singapore: World Scientific), 261
 Jones, L. 1990, in *Proc. 21st Int. Cosmic Ray Conf. (Adelaide)*, 2, 75
 Jones, T. W., & Kang, H. 1992, in *AIP Conf. Proc.* 264, *Particle Acceleration in Cosmic Plasmas*, ed. G. Zank & T. Gaisser (New York: AIP), 148
 Kosack, K., et al. 2004, *ApJ*, 608, L97
 Krennrich, F., et al. 2004, *NewA Rev.*, 48, 345
 Lagage, P. O., & Cesarsky, C. J. 1983, *A&A*, 125, 249
 Longair, M. S. 1994, *High Energy Astrophysics*, Vol. 2 (2nd ed.; Cambridge: Cambridge Univ. Press)
 Maeda, Y., et al. 2002, *ApJ*, 570, 671
 Markoff, S., Melia, F., & Sarcevic, I. 1997, *ApJ*, 489, L47
 ———. 1999, *ApJ*, 522, 870
 Mayer-Hasselwander, H., et al. 1998, *A&A*, 335, 161
 Medina-Tanco, G. A., & Watson, A. A. 2001, in *Proc. 27th Int. Cosmic Ray Conf. (Hamburg)*, 2, 337
 Melia, F., & Falcke, H. 2001, *ARA&A*, 39, 309
 Melia, F., et al. 1998, *ApJ*, 508, L65
 Moskalenko, I. V. 1995, *Space Sci. Rev.*, 72, 593
 Mucke, A., et al. 1999, *Publ. Astron. Soc. Australia*, 16, 160
 Ostapchenko, S. S. 2003, *J. Phys. G*, 29, 831
 Parker, E. N. 1965, *Planet. Space Sci.*, 13, 9
 Pedlar, A., et al. 1989, *ApJ*, 342, 769
 Shklovskii, I. S. 1953, *Dokl. Akad. Nauk SSSR*, 91, 475
 Sikora, M., Begelman, M. C., & Rudak, B. 1989, *ApJ*, 341, L33
 Stecker, F. W. 1979, *ApJ*, 228, 919
 Takahashi, K., & Nagataki, S. 2001, preprint (astro-ph/0108507)
 Takeda, M. 1999, in *26th Int. Cosmic Ray Conf. (Salt Lake City)*, 3, 252
 Telesco, C. M., Davidson, J. A., & Werner, M. W. 1996, *ApJ*, 456, 541
 Thompson, D. J. 2004, *NewA Rev.*, 48, 543
 Tkaczyk, W. 1994, *ApJS*, 92, 611
 Tsuchiya, K., et al. 2004, *ApJ*, 606, L115
 Werner, K. 1993, *Phys. Rep.*, 232, 87
 Wolfire, M. G., Tielens, A. G. G. M., & Hollenbach, D. 1990, *ApJ*, 358, 116
 Yusef-Zadeh, F., et al. 1996, *ApJ*, 466, L25
 ———. 1999, *ApJ*, 527, 172